Computer prediction and genetic analysis identifies retinoic acid modulation as a driver of conserved longevity pathways in genetically-diverse *Caenorhabditis* nematodes

Stephen A. Banse[1], Christine A. Sedore[1], Anna L. Coleman-Hulbert[1], Erik Johnson[1], Brian Onken[2], David Hall[3], Erik Segerdell[1], E. Grace Jones[1], Yuhua Song[2], Hadley Osman[3], Jian Xue[2], Elena Battistoni[3], Suzhen Guo[2], Anna C. Foulger[3], Madhuri Achanta[2], Mustafa Sheikh[3], Theresa Fitzgibbon[3], John H. Willis[1], Gavin C. Woodruff[1#], Monica Driscoll[2], Gordon J. Lithgow[3], Patrick C. Phillips[1*]

Abstract Aging is a pan-metazoan process with significant consequences for human health and society—discovery of new compounds that ameliorate the negative health impacts of aging promise to be of tremendous benefit across a number of age-based comorbidities. One method to prioritize a testable subset of the nearly infinite universe of potential compounds is to use computational prediction of their likely anti-aging capacity. Here we present a survey of longevity effects for 16 compounds suggested by a previously published computational prediction set, capitalizing upon the comprehensive, multi-species approach utilized by the *Caenorhabditis* Intervention Testing Program (CITP). While eleven compounds (aldosterone, arecoline, bortezomib, dasatinib, decitabine, dexamethasone, erlotinib, everolimus, gefitinib, temsirolimus, and thalidomide) either had no effect on median lifespan or were toxic, five compounds (all-trans retinoic acid, berberine, fisetin, propranolol, and ritonavir) extended lifespan in *Caenorhabditis elegans*. These computer predictions yield a remarkable positive hit rate of 30%. Deeper genetic characterization of the longevity effects of one of the most efficacious compounds, the endogenous signaling ligand all-trans retinoic acid (atRA, designated tretinoin in medical products), which is widely prescribed for treatment of acne, skin photoaging and acute promyelocytic leukemia, demonstrated a requirement for the regulatory kinases AKT-1 and AKT-2. While the canonical Akt-target FOXO/DAF-16 was largely dispensable, other conserved Akt-targets (Nrf2/SKN-1 and HSF1/HSF-1), as well as the conserved catalytic subunit of AMPK AAK-2, were all necessary for longevity extension by atRA. Evolutionary conservation of retinoic acid as a signaling ligand and the structure of the downstream effector network of retinoic acid combine to suggest that the all-trans retinoic acid pathway is an ancient metabolic regulatory system that can modulate lifespan. Our results highlight the potential of combining computational prediction of longevity interventions with the power of nematode functional genetics and underscore that the manipulation of a conserved metabolic regulatory circuit by co-opting endogenous signaling molecules is a powerful approach for discovering aging interventions.

Affiliations: [1]Institute of Ecology and Evolution, University of Oregon, Eugene, OR 97403, USA; [2]Rutgers University, Dept. of Molecular Biology and Biochemistry, Piscataway, NJ, 08854, USA; [3]The Buck Institute for Research on Aging, Novato, CA, 94945, USA; [#]Current affiliation - University of Oklahoma, Dept. of Biology, Norman, OK 73019, USA. *Corresponding author E-mail: pphil@uoregon.edu

Key Terms: *Caenorhabditis elegans*, *Caenorhabditis briggsae*, *Caenorhabditis tropicalis*, CITP, all-trans retinoic acid, propranolol, arecoline, bortezomib, dasatinib, decitabine, dexamethasone, erlotinib, everolimus, gefitinib, temsirolimus, thalidomide, aldosterone, berberine, fisetin, ritonavir, metoprolol, longevity, healthspan, computational predictions, *aak-2*, *akt-1*, *akt-2*, *daf-16*, *eat-2*, *hsf-1*, *pmk-1*, *skn-1*, *tol-1*, RNAseq

Introduction

Aging is a primary risk factor for a myriad of chronic illnesses, health declines, and mortality. A central premise of research in the current aging field is that aging *per se* can be treated directly, leading to ancillary benefits across a broad range of age-related comorbidities (the "geroscience hypothesis"; Austad, 2016; Kennedy et al., 2014). But how best to identify compounds holding the potential for broad-spectrum effects across an individual's lifespan? While comprehensive screens using model organisms such as the nematode *Caenorhabditis elegans* provide a good approach (Petrascheck et al., 2007), a complementary alternative is to use emerging databases of compound-specific physiological effects to predict which compounds are most likely to lead to positive effects on extending lifespan (Janssens et al., 2019; Ribeiro et al., 2023). An advantage of this approach is that the predictive models should become better and better as the training set of positive hits continues to expand over time (Vanhaelen et al., 2020; Zhavoronkov et al., 2019). Still, the efficacy of any predictive model is strongly dependent on the quality of the input data, and the well-documented heterogeneity of aging as a phenotype, as well as general challenges in reproducibility *per se*, create barriers to the successful application of predictive approaches to aging research. The *Caenorhabditis* Intervention Testing Program (CITP) tests compounds for lifespan and healthspan effects across a genetic diversity panel of *Caenorhabditis* nematode strains (Lucanic et al., 2017). Beyond *robustness* of response across genetic backgrounds, the CITP has painstakingly focused on *reproducibility* across laboratories and trials via standardization of methods and a hierarchical statistical approach that accounts for experimental variation at a variety of levels of replication. These features make the CITP an ideal framework for testing computer predictions of longevity interventions and serve as the foundation for data collection for improved models in the future.

As a first step toward testing the efficacy of computational prediction of lifespan extending compounds, we used a previously published set of compound predictions developed via an analysis of the overlap of drug-induced and aging-related gene expression and protein interactions (Fuentealba et al., 2019) to develop a list of candidate compounds for further investigation using the CITP workflow. We prioritized compounds with the highest predictive scores and

eliminated several compounds whose effects in *C. elegans* were already well characterized. Our analysis led to a set of 16 compounds (aldosterone, all-trans retinoic acid (atRA), arecoline, berberine, bortezomib, dasatinib, decitabine, dexamethasone, erlotinib, everolimus, fisetin, gefitinib, propranolol, ritonavir, temsirolimus, and thalidomide) selected for further testing. As outlined below, we found that of the five candidate compounds—atRA, berberine, fisetin, ritonavir, and propranolol—that extended median lifespan, propranolol and atRA conferred the largest positive effects. Potential confounding interactions of propranolol with the bacterial food of the nematodes led us to focus on atRA for more in-depth genetic and functional analysis.

atRA is an FDA approved intervention used topically in dermatology and systemically as a chemotherapeutic adjuvant (Giuli et al., 2020; Szymański et al., 2020). Endogenously, atRA is the most bioactive retinoid derived from vitamin A, known to function as a highly conserved signaling ligand involved in transcriptional regulation (Albalat, 2009; Albalat and Cañestro, 2009; Fonseca et al., 2020). In *C. elegans*, the presence of vitamin A metabolism pathway genes (Kostrouch et al., 1995; Yilmaz and Walhout, 2016) (Supplemental figure 1A), metabolism of exogenous vitamin A into retinal and atRA (Chen et al., 2018), known affinity of *C. elegans* fatty acid- and retinol-binding proteins for retinoids (Garofalo et al., 2003), and endogenous atRA detection in untreated animals (Chen et al., 2018) combine to suggest the presence of an endogenous nematode atRA signaling pathway. While conservation of the ligand atRA is well supported, the canonical vertebrate downstream retinoid receptors (RXR and RAR) that effect transcriptional responses have not been identified in nematodes. In contrast with the elusive retinoic acid receptors, however, the mammalian kinases modulated by atRA have extensively studied *C. elegans* orthologs (Supplemental figure 1B). In humans, atRA modulates transcription via PI3K/Akt (Bastien et al., 2006; Ben-Sasson et al., 2011; Farias et al., 2005; García-Regalado et al., 2013; Lee et al., 2014; Masiá et al., 2007; Qiao et al., 2012) and p38 MAPK (Alsayed et al., 2001; De Genaro et al., 2013; Hormi-Carver et al., 2007; Lee et al., 2008; Roe et al., 2020; Shinozaki et al., 2007) kinase signaling. Functionally, kinase signaling is likely mediated by atRA regulation of the kinase phosphorylation state, as has been shown for Akt in mammalian (Bastien et al., 2006; García-Regalado et al., 2013; Qiao et al., 2012) and avian (Yu et al., 2012) cell culture.

Building upon our general screening approach, we present a more comprehensive genetic analysis of atRA impact on longevity that suggests functional conservation of atRA kinase regulation, as the effects of atRA on longevity requires kinases encoded by both *akt-1* and *akt-2*. In *C. elegans* and mammals, Akt kinases regulate powerful aging pathways (e.g., insulin-like signaling (IIS), FOXO, Nrf2). Our genetic analysis of atRA longevity in *C. elegans* suggests that the FOXO/DAF-16 transcription factor is not necessary, consistent with atRA acting downstream of, or in parallel to, FOXO. In contrast to FOXO/DAF-16, the Akt-phosphorylation targeted Nrf2 homolog SKN-1 and heat shock transcription factor 1 homolog HSF-1, along with the conserved catalytic subunit of the energy sensor AMPK AAK-2, are required for atRA-induced lifespan extension. The conservation of atRA as a signaling molecule, and the pathways through which atRA affects metabolism and lifespan, anchor the prediction that all-trans retinoic acid intervention (or atRA chemical variants) will translate into efficacious anti-aging in future mammalian and clinical studies.

Results

Experimental testing of computational predictions identifies all-trans retinoic acid as a candidate pro-longevity intervention

To select compounds for CITP testing (Figure 1A), we began with the top 10% of candidates from a published list of computationally ranked compounds built using known drug-protein interactions (Fuentealba et al., 2019). To avoid duplicative effort and to favor novel discovery, we used the DrugAge database (Barardo et al., 2017b) to de-prioritize compounds that had already been published to extend *C. elegans* lifespan. We then selected 16 candidate interventions by cross-referencing the remaining compounds with the top 10% of two additional computational efforts that predicted aging effects based on comparative transcriptional responses (Janssens et al., 2019) (all-trans retinoic acid, arecoline, propranolol, thalidomide) and machine-learning models based on gene ontologies and physical structures (Barardo et al., 2017a) (aldosterone, berberine, bortezomib, dasatinib, decitabine, dexamethasone, erlotinib, gefitinib, ritonavir, temsirolimus), or listing in the DrugAge database with published lifespan extension in other systems (everolimus (Spindler et al., 2012), fisetin (Yousefzadeh et al., 2018)).

The selected compounds comprise a number of common aging-related classes, including bortezomib (a proteasome inhibitor; Chen et al., 2011), fisetin (a sirtuin activator; Kim et al., 2015), temsirolimus (a PI3K/mTOR inhibitor and derivative of rapamycin; Ali et al., 2022), and dasatinib (a tyrosine kinase inhibitor; Talpaz et al., 2006), among others (Table 1). We then screened the selected compounds at 4-5 concentrations using full lifespan analysis (Figure 1 figure

supplement 1). Among the 16 candidate interventions, three were water soluble and thirteen were DMSO soluble. While DMSO can impact lifespan (Wang et al., 2010), we did not observe a difference between the H_2O and DMSO vehicle control treatments (median lifespan 17 days for both, *p*=n.s.), consistent with the published absence of DMSO effects at concentrations similar to those used in our studies (AlOkda and Van Raamsdonk, 2022). Among the 16 computationally prioritized candidate compounds, we found that aldosterone, dexamethasone, erlotinib, decitabine, dasatinib, everolimus, thalidomide, and temsirolimus did not significantly change median lifespan at any tested concentration (Figure 1B; Figure 1 figure supplement 1).

Among the eight remaining candidates, we found that three compounds shortened median lifespan (arecoline, gefitinib, and bortezomib). Tests of muscarinic/nicotinic agonist arecoline at five concentrations ranging from 50 μM to 8 mM revealed toxic effects at the highest concentration (-29.4% median lifespan, $p<0.0001$). The epidermal growth factor inhibitor gefitinib also had small, but significant, negative effects at 10, 25, 50, and 80 μM (Figure 1 figure supplement 1). In contrast, the 26S proteosome inhibitor bortezomib conferred strong toxicity effects that increased with concentration through the entire concentration range we tested (5, 10, 20, and 30 μM, -10.5% to -47.3% median lifespan; $p=0.0002$ at 5 μM and $p<0.0001$ at all other concentrations; Figure 1 figure supplement 1). Thus, some compounds computationally predicted to enhance longevity can be found to be toxic when empirically investigated, underscoring that validation is a key element of any prediction pipeline.

We found that the remaining five compounds conferred statistically significant positive effects on median lifespan for at least one tested concentration (Figure 1B; Figure 1 figure supplement 1), representing a hit success rate of 31.25% (5/16) for our test set (Table 1). Seven additional compounds met our selection criteria, but because they had been previously tested by the CITP, we did not include these compounds in tests presented here (see Table 1). With those previously-tested compounds included, we see a similar overall hit success rate of ~30% (7/23) (Table 1). The bio-activity of these compounds were as follows: ritonavir had effects at 20 and 35 μM (6.3%, $p=0.0016$ and $p=0.0282$ respectively). The sirtuin activation/mTOR inhibitor fisetin had positive effects at 10, 50, and 100 μM ($p=0.0081$, p=0.0025, and $p=0.0032$, respectively), with an effect size up to 11.8%, and no effect detected at 20 μM. The AMPK activator berberine conferred significant effects only at 100 μM, with an 11.8% increase in median lifespan ($p<0.0001$). In support of the potential translatability of the computationally-predicted candidate compounds tested here, fisetin (Yousefzadeh et al., 2018) and berberine (Dang et al., 2020) have also been found to increase median lifespan in mice.

The two remaining candidate interventions induced large increases in longevity, with propranolol extending median lifespan 44.4% at 1 mM ($p<0.0001$) and atRA extending median lifespan 23.5% at 150 μM ($p<0.0001$) (Figure 1B). Propranolol and atRA are particularly interesting interventions because they are both FDA approved drugs, potentially providing an easier path toward clinical use as aging interventions. For example, propranolol is a well-tolerated drug with a long history of use (Srinivasan, 2019, p. 50; Zacharias et al., 1972) treating high blood pressure (Prichard and Gillam, 1964), angina (Hamer et al., 1964), and atrial fibrillation (Rowlands et al., 1965). While we observed a large (44.4%, $p<0.0001$) median lifespan extension at 1 mM propranolol, we also saw extension at 0.5 mM (16.7%, $p<0.0001$) (Figure 2D). In contrast to the positive effects that we observed at 0.5 and 1 mM, we found that increasing the treatment concentration to 5 mM propranolol resulted in toxicity and a reduction in lifespan (-61.1%, $p<0.0001$) (Figure 2D). These observations led us to extend our tests into the related species *C. briggsae* (AF16) and *C. tropicalis* (JU1630). In these two species, we observed similar toxicity at 5 mM ($p<0.0001$), but no beneficial effects at lower concentrations (Figure 2E and F).

In human applications, propranolol functions as a general antagonist of β1 and β2 beta-adrenergic receptors. We therefore sought to determine if a β1 specific antagonist like metoprolol could recapitulate the longevity effects in *C. elegans*. We assayed longevity effects for metoprolol across a concentration range of 5 μM-1.5 mM and observed no positive effects (Figure 2 figure supplement 2A). Although there could be multiple reasons that metoprolol was not effective, we followed up by asking whether the effects of propranolol require β2 antagonism or are unrelated to β-adrenergic antagonism. A β-adrenergic-independent mechanism was suggested by the change we noted in the appearance of the bacterial lawns on propranolol-treated plates. When we tested bacterial growth, we found that propranolol reduced bacterial growth at the same concentrations at which we observed lifespan effects (Figure 2 figure supplement 2C). The propranolol impact on bacterial food source growth suggests a potential indirect food-dependent mechanism for propranolol on *C. elegans* lifespan. We therefore repeated the lifespan studies at 0.5 mM and 1 mM in the presence of paraformaldehyde-treated bacteria that are metabolically inert (Beydoun et al., 2021). Under conditions in which propranolol effects on bacterial growth were eliminated, we observed shorter lifespans in populations treated by propranolol (Figure 2 figure supplement 2B). These observations suggest that propranolol either does not exert direct

beneficial effects on lifespan in *C. elegans* or has confounding direct and indirect effects that depend on bacterial food state. The potential food-dependent effects of propranolol require further study beyond the scope of our current screening protocols. Therefore, we elected to focus on the large lifespan extension generated by atRA treatment for the remainder of this study.

Longevity extension via atRA treatment is dependent upon genetic background

The scientific literature is rife with examples of intervention effects on longevity that vary in response to experimental differences. Indeed, previous experiments treating *C. elegans* with atRA have resulted in contradictory effects (Janssens et al., 2019; Statzer et al., 2021) for reasons that are not entirely clear. To determine the most efficacious concentration of atRA treatment, we tested a dosage range from 1 μM to 150 μM. For *C. elegans* N2, we observed increasing positive effects at all tested concentrations above 1 μM (which had no detectible effect; Figure 2) and a very slight but significant increase in median lifespan for *C. tropicalis* JU1630 at 150 μM atRA (7.7%, p=.0215). However, we observed no effects in *C. briggsae* across the tested concentration range (Figure 2B). Given these observations, we elected to use 150 μM atRA for the remainder of the experiments in this study. In contrast with propranolol, we observed no obvious effects of atRA on bacterial growth using replica plating.

Expanding this analysis across a more extensive genetic diversity set following the full CITP replication protocol, we tested the effects of atRA on three strains of *C. elegans* (N2, JU775, MY16), *C. briggsae* (AF16, ED3092, HK104), and *C. tropicalis* (JU1630, JU1373, QG834) (Figure 3) with replication at three distinct geographic sites (University of Oregon, Rutgers University, and the Buck Institute). Total genetic variation across *C. elegans* strains is comparable to that observed among humans, while the differences among species are comparable to the genetic distance between humans and mice (Teterina et al., 2022). We found that the substantial atRA-associated effects on longevity are robust to genetic variation across all three *C. elegans* strains, yielding lifespan extensions of 18.8-44.4% (Figure 3; Figure 3 figure supplement 1A). While the lifespan extension initially observed in *C. tropicalis* JU1630 failed to replicate, *C. tropicalis* QG834 displayed a small but significant increase in lifespan (Figure 3; Figure 3 supplement 1C). Clearly, given the small effect size, we are at the edge of statistical power to detect a positive effect within this species. Again, atRA did not register any significant positive effects in the *C. briggsae* strains (Figure 3; Figure 3 figure supplement 1B). Partitioning total variation across this large set of experimental replicates, we found only a small amount of variability attributable to site (3.8%) or differences among experimenters (7.3%), with the majority of variance being attributable to individual variation (56.1%; Figure 3 figure supplement 2), consistent with previous CITP studies (Banse et al., 2024c; Lucanic et al., 2017). Thus, atRA treatment is reproducible within and between laboratories, but subject to high levels of individual variation, as are all longevity studies.

To increase the temporal resolution of our survivorship curves, we repeated our longevity analyses using the Automated Lifespan Machine (ALM) technology (Stroustrup et al., 2013) across the same nine genetically diverse strains. We again observed a positive effect for the three *C. elegans* strains, demonstrating the robustness of atRA longevity effects across genetic backgrounds in these strains (Figure 3 figure supplement 3). Interestingly, we do not see any positive effects of atRA on the ALM for *C. briggsae* or *C. tropicalis*, but instead see slightly toxic effects for *C. briggsae* strains AF16 and HK104 and *C. tropicalis* strain JU1630. It is not clear what might drive this difference, although the ALM introduces some different environmental stresses and conditions as compared to manual assay conditions (for example, repeated light exposure and distinct compound introduction; see Banse et al. (2019) for discussion).

atRA tends to enhance locomotory healthspan in C. elegans*, but not in* C. briggsae *or* C. tropicalis

A goal of longevity interventions is to enhance physiological health, which, like in humans, can be measured as improvement in older age locomotory capacity. We therefore determined the effect of atRA exposure on aging adult swim performance using a video analysis of swimming behavior (Ibáñez-Ventoso et al., 2016; Restif et al., 2014). In previous work, we reported that anti-aging interventions can have disparate effects on longevity and adult swimming ability and that treated strains can show positive effects in motility enhancement (Banse et al., 2024b) even in the absence of longevity enhancement. Using strain-specific models for swimming behavior to generate a composite swimming score based on eight underlying measures (Banse et al., 2024b), we observed significant improvement for two of the *C. elegans* strains at day 12 of adulthood (Figure 3 Figure supplement 4). Similar to atRA effects on longevity, we find that atRA was generally ineffectual at promoting swimming health in *C. briggsae* and *C. tropicalis*, with improvements only seen in day 16 of AF16 (41.6%, p=0.00191), while decreased swimming scores were observed in all three *C. tropicalis* strains at one or more test days. Overall, then, atRA has largely positive effects on *C. elegans*

longevity and health while it has the potential to be detrimental to *C. briggsae* and *C. tropicalis* depending on the assay type and particular genetic background.

atRA lifespan extension requires atRA-modulated kinases AKT-1, AKT-2, and AMPK

Given the plasticity of genetically-determined longevity within *C. elegans*, we next sought to identify the pathways required for atRA lifespan extension. Because no retinoic acid binding transcription factors have been identified in *C. elegans*, we looked to the known effects of atRA in modulating human kinase activity (Albalat, 2009; Albalat and Cañestro, 2009; Fonseca et al., 2020) to identify candidate pathways. The vertebrate atRA responsive kinases do have extensively studied orthologs in *C. elegans* (Supplemental figure 1B). Akt-homologs emerged as particularly relevant due to their involvement in longevity-related IIS signaling, and the fact that in mammals phosphorylation of Akt in response to atRA occurs at a site that appears to be conserved in the *C. elegans* Akt homologs (García-Regalado et al., 2013) (Supplemental figure 1C). We therefore asked whether either *akt-1* or *akt-2* were required for atRA lifespan effects by measuring the lifespans of *akt-1(ok525)* and *akt-2(ok393)* loss of function mutants (Figure 4A,B). Consistent with previously published studies (Newell Stamper et al., 2018; Soukas et al., 2009), in control treated animals we observed longer median lifespans for the mutants (median 26 and 23 days versus 17 in WT). When we performed longevity analysis of *akt-1(ok525)* in the presence of atRA (Figure 4A), we observed a significant decrease in longevity (-7.7% median lifespan, p=0.00000142), demonstrating a requirement for AKT-1 in atRA-induced longevity extension. Repeating the analysis in *akt-2(ok393)* mutants (Figure 4B) demonstrated a complete dependence on AKT-2, with atRA having no significant effect in the *akt-2* mutant background (p=0.7170). We conclude that atRA longevity effects require *akt-1* and *akt-2,* consistent with a known atRA signaling mechanism in mammals.

Similarly, in human cell culture (Ishijima et al., 2015) and mouse models (Zhang et al., 2019), retinoic acid activates AMPK. AMPK is a conserved sensor of intracellular energy state that regulates glucose and lipid metabolism. Previous work has shown that AMPK is involved in the transition to gluconeogenesis in the long-lived dauer stage (Penkov et al., 2020) and may also play a role in gluconeogenesis in adults (Nguyen et al., 2020). In *C. elegans,* AMPK is required for many longevity interventions (Jayarathne et al., 2020; Onken and Driscoll, 2010; Peng et al., 2019), while overexpression of the AMPK catalytic subunit *aak-2* (Apfeld et al., 2004)*,* or expression of a constitutively activated AAK-2 (Greer et al., 2007; Mair et al., 2011), can directly increase lifespan. Additionally, AMPK both regulates, and is regulated by, Akt, making AMPK an interesting candidate for involvement in atRA longevity effects. We therefore tested *aak-2(ok524)* mutants for atRA lifespan extension. We observed that the atRA lifespan extension was fully dependent on *aak-2* (Figure 4C). Overall, our data suggest that atRA longevity may be mediated through a conserved signaling process.

Robust atRA lifespan extension requires the HSF-1 and SKN-1 transcription factors

Another set of atRA transducing factors signaling are *hsf-1,* the human heat shock factor 1 transcription factor homolog, and *skn-1,* the nematode homolog of the mammalian Akt-target Nrf2. Previous work has demonstrated that HSF-1 is required for several lifespan extending genetic and pharmacological interventions in *C. elegans* (Lazaro-Pena et al., 2022; Steinkraus et al., 2008; Todorova et al., 2023) and that *skn-1* can directly promote lifespan (Tang and Choe, 2015; Tullet et al., 2017), as well as being implicated in multiple longevity interventions (Duangjan et al., 2019; H. W. Seo et al., 2015) including vitamin D (Mark et al., 2016) and thioflavin T (Alavez et al., 2011; Lucanic et al., 2017). In mammalian studies, Akt directly regulates HSF1 through phosphorylation (Carpenter et al., 2015; Da Costa et al., 2020; Lu et al., 2022; Tang et al., 2020), and *hsf-1* has been implicated as a downstream effector of PI3K/Akt signaling that functions in conjunction with DAF-16 to regulate lifespan in *C. elegans* (Chiang et al., 2012; Hsu et al., 2003). We tested for atRA lifespan extension in a *hsf-1(sy441)* mutant encoding a premature stop codon that removes the conserved transactivation domain (Hajdu-Cronin et al., 2004). In this *hsf-1* background, atRA treatment had a greatly reduced impact on lifespan, showing only a small increase in median lifespan and no extension in maximum lifespan (Figure 4D).

Because *skn-1* is an essential gene required developmentally to specify mesodermal fates (Bowerman et al., 1992; Maduro et al., 2001), we tested for longevity effects of atRA in animals fed HT115 *E. coli* carrying an RNAi vector targeting *skn-1* (Kamath and Ahringer, 2003) starting from the L3/L4 developmental stage (*skn-1* is an essential gene for early development, and thus assaying a knockout mutation or beginning with earlier interventions is not possible). It should be noted that we observed that the HT115 strain of *E. coli* itself extends lifespan relative to strain OP50, consistent with previous findings (Stuhr and Curran, 2020) (Figure 4 Figure supplement 1B). When we compared *skn-1* RNAi treated animals exposed to atRA versus vehicle control, in contrast to the lifespan extension for animals under

control RNAi conditions, we observed a 23.8% decrease in median lifespan ($p<0.001$) (Figure 4E and Figure 4 Figure supplement 1B), suggesting that atRA is toxic in the absence of *skn-1* function. Our data are consistent with *hsf-1* and *skn-1* being necessary for the lifespan-extending transcriptional response to atRA and/or for addressing potential toxic side effects of atRA.

The FoxO/DAF-16 transcription factor is not essential for atRA lifespan extension

Given the dependence on *akt-1/2*, we sought to determine if atRA lifespan extension requires the canonical *C. elegans* AKT-target *daf-16*/FOXO, a known regulator of aging (Murphy and Hu, 2013) for which activation is a common feature of chemical interventions that extend *C. elegans* lifespan (Kim et al., 2019; Wang et al., 2015; Zhao et al., 2017) (although *daf-16* independent lifespan extension is also possible; (Onken and Driscoll, 2010). We therefore measured longevity in *daf-16(mu86)* null mutants treated with atRA. We found that *daf-16(mu86)* animals still exhibited a lifespan extension (12%, $p<0.0001$) compared to vehicle control animals (Figure 4F). The fact that the atRA longevity effect size is larger in wildtype animals (24% vs 12%), reveals that although *daf-16* contributes in part to the atRA effect, DAF-16 is not absolutely required, and therefore additional or alternative outputs must be operative. Inputs to longevity pathways are well documented to be complex and inter-related (Narasimhan et al., 2009; Nikoletopoulou et al., 2014; Parkhitko et al., 2020). For example, *akt-1* and *akt-2* are primary upstream modulators of *daf-16* in the IIS pathway regulation of the long-lived alternative dauer larval state (Paradis and Ruvkun, 1998), but have little effect on IIS modulation of adult longevity, when *sgk-1* becomes the primary regulator of DAF-16 (Hertweck et al., 2004). We conclude that atRA acts in part via DAF-16 but infer that atRA either acts independently of the IIS pathway, or primarily through the PI3K/Akt portion of the IIS pathway, which would be consistent with Akt-dependent atRA signaling in mammals (Bastien et al., 2006; García-Regalado et al., 2013; Qiao et al., 2012).

atRA lifespan extension in **tol-1** *and* **pmk-1** *mutants*

While our observation that atRA requires AKT-1/2 and SKN-1 is consistent with a simple signaling cascade in which atRA modulates Akt regulation of SKN-1, more complicated responses are possible. Previous research has established that there is crosstalk between Akt and p38 MAPK signaling in humans (Gonzalez et al., 2004) and in *C. elegans* (Tullet et al., 2009). Genetic and biochemical analysis of SKN-1 has shown that in addition to Akt regulation, SKN-1 is also post-translationally regulated by the *pmk-1*/p38 MAPK pathway (Figure 4 figure supplement 1A). Importantly, work in mammals has implicated p38/MAPK signaling in atRA responses (Alsayed et al., 2001; De Genaro et al., 2013; Hormi-Carver et al., 2007; Lee et al., 2008; Roe et al., 2020; Shinozaki et al., 2007), suggesting that atRA may affect two different signaling cascades that can regulate SKN-1.

In light of these considerations, we addressed p38 MAPK signaling as a potential effector pathway for atRA. *C. elegans* has three known p38 mitogen-activated protein kinase homologs*, pmk-1, pmk-2,* and *pmk-3*. SKN-1 is regulated by the MAPK cascade that culminates with p38/PMK-1 phosphorylation of SKN-1 at serines 164 and 430 (Figure 4 Figure supplement 1A). The phosphorylation of S164 and A430 sites results in increased nuclear SKN-1 levels, resulting in transcription of innate immunity and oxidative stress genes (Inoue et al., 2005). When we tested *pmk-1(km25)* mutants for atRA longevity effects, we found that *pmk-1(km25)* mutants exhibit an atRA-induced extension in median lifespan (26.3%, $p<0.0001$), but did not exert an effect on maximum lifespan, suggesting enhanced importance of *pmk-1* later in life (Figure 4G). Although our data identify AKT-1 and AKT-2 as more impactful than p38/PMK-1 in atRA-mediated longevity, additive and more complex atRA regulation of SKN-1 by PI3K/Akt and p38 MAPK pathways may be possible. For example, Akt regulates SKN-1 through phosphorylation of serine 12 (Blackwell et al., 2015), while *pmk-1* regulates SKN-1 through serines 164 and 430 (Figure 4 figure supplement 1A).

To probe the candidate signaling pathways further, we considered potential pathway receptors. *C. elegans PMK-1* functions downstream of *TIR-1* (Liberati et al., 2004; Peterson et al., 2022), one of two Toll/interleukin-1 receptor homology (TIR) domain-containing genes (Paysan-Lafosse et al., 2023). The second TIR-domain containing protein is the membrane associated TOL-1, which signals through a p38 MAPK cascade including *mom-3* and *pmk-3*, and ultimately IKB-1. We measured the lifespan of *tol-1(nr2033)* mutants treated with atRA to find that *tol-1(nr2033)* animals exhibit an enhanced response to atRA, with an 82.4% increase in median lifespan in the mutant background relative to the 23.5% increase observed in the N2 wildtype background (Figure 4H).

atRA can extend lifespan in a genetic caloric restriction model

One widely conserved mechanism for lifespan extension is caloric restriction. In *C. elegans* longevity research, one frequently used caloric restriction model is genetic mutation of *eat-2*. EAT-2 is a nicotinic acetylcholine receptor expressed in the pharyngeal muscle that facilitates normal, fast feeding behavior (Avery, 1993; McKay et al., 2004;

Raizen et al., 1995). In an *eat-2* mutant background, feeding behavior is slowed, inducing a caloric restriction state that extends life (Lakowski and Hekimi, 1998), either via dietary restriction itself or via a combination of dietary restriction and an innate immunity response to altered bacterial processing (Kumar et al., 2019). Previous work has shown that some compound interventions are incapable of further prolonging *eat-2* lifespan (e.g., metformin; Onken and Driscoll, 2010), while other interventions appear independent/additive (e.g., Sonneradon A; Jiang et al., 2022) with *eat-2* effects. We were particularly interested in the possibility that atRA might act as an *eat-2*-like dietary restriction mimetic because previous characterization demonstrated that *eat-2* longevity was independent of *daf-16* (Lakowski and Hekimi, 1998), but dependent on *skn-1* (Park et al., 2010), mimicking our observations for atRA. We therefore treated *eat-2(ad1113)* mutants with vehicle and atRA. Consistent with atRA acting through a mechanism distinct from *eat-2*, we observed a significant atRA induced extension in lifespan in the *eat-2(ad1113)* animals (36.8% increase in median survival, p<2e-16) (Figure 4I). In *C. elegans* studies, caloric restriction can be induced through several different experimental regimes, each of which requires a different set of genetic pathways to exert longevity effects (Greer and Brunet, 2009). We therefore conclude that atRA longevity effects are either unrelated to and/or are mechanistically distinct from *eat-2* effects on longevity.

atRA treatment alters gene expression in stress response pathways

Given the dependency of lifespan extension under atRA treatment, we used RNAseq to assess transcriptional changes under atRA treatment in wildtype N2 animals. We performed RNAseq on day four adult animals treated with atRA compared to carrier control. We were able to detect the expression of 12,746 *C. elegans* genes in our dataset (Figure 5A). Among the detected genes, 17% (2,169) were differentially expressed with atRA treatment (*FDR*<.05). We defined the subset of differentially expressed genes with an absolute $\log_2$ fold change (LFC) greater than one as wildtype atRA response genes (WaRGs). The WaRGs represent ~5.1% of all detected genes (653 total) and were more heavily weighted towards downregulated genes, with 487 (3.8% of total) downregulated versus 166 (1.3% of total) upregulated. Analysis of the expression pattern of the WaRGs shows a skewed distribution among the upregulated genes, with 86% (138/160; q=5.9e-38) of the genes with characterized expression being produced in the intestine. The downregulated genes are enriched for genes expressed in the excretory duct (32/470; q=4.1e-9), excretory socket cell (29/470; q=5.1e-08), and the epithelial system (281/470; q =2.7e-8). Potentially relevant to metabolic regulation of aging, the intestine and the hypodermal cells are the primary energy storage tissues in *C. elegans* (Mak, 2012; Mullaney and Ashrafi, 2009).

A WormCat 2.0 (Higgins et al., 2022; Holdorf et al., 2020) enrichment analysis of the WaRGs (Figure 5B) showed overlapping and differing enrichments between up- and down-regulated genes. For example, we noted stress-related gene enrichments in both classes of WaRGs, consistent with known PI3K/Akt and p38 MAPK functions in *C. elegans* and with the strong correlation between stress response and longevity (Zhou et al., 2011). Among the non-overlapping enrichments, we found that the upregulated set was enriched for metabolism and transmembrane transport genes (Figure 5B). We found that collagen and neuropeptide related genes (Figure 5B) were disproportionally represented among the non-overlapping but downregulated set. We were particularly surprised by the former because atRA was identified as a longevity modulator through induction of a collagen (*col-144::gfp)* reporter (Statzer et al., 2021) and some observations correlate longevity with collagen expression (Ewald et al., 2015; Goyala and Ewald, 2023). Separation of the collagen and collagen-related genes by type (Teuscher et al., 2019) demonstrated a general trend of atRA either not changing, or downregulating, collagen genes (Figure 5 figure supplement 1). For example, the cuticular collagens, of which *col-144* is a predicted member, and other core genes associated with the extracellular matrix (matrisome genes) were either unchanged in expression or down regulated (Figure 5 figure supplement 1). In contrast with the core-matrisome genes, the matrisome-associated category did include a number of upregulated genes in the ECM-regulator and ECM-affiliated subclasses.

We also analyzed the WaRGs from a metabolic perspective using the WormFlux Pathway enrichment tool (Walker et al., 2021). Among the 166 upregulated WaRGs we documented an enrichment of sphingolipid metabolism (8/45 genes, $p_{\text{enrichment}}$=2.3e-07) (Figure 5 figure supplement 2) and iron metabolism (2/15 genes, $p_{\text{enrichment}}$=0.025) pathway genes, while the 487 downregulated WaRGs were enriched for fatty acid biosynthesis (6/24 genes, $p_{enrichment}$=0.00051), fatty acid degradation (2/8 p=0.048), folate biosynthesis (2/8 genes, $p_{\text{enrichment}}$=.048), and UGT enzyme (8/67, $p_{\text{enrichment}}$=0.0094) pathway genes. Interestingly, WormFlux analysis also suggests that genes related to the electron transport chain may be under-represented (0/88 genes, $p_{depletion}$=0.013) among the downregulated WaRGs.

Because of the potential overlap of enriched gene categories with the functions of the IIS-PI3K/Akt and Nrf2-p38 MAPK pathways in *C. elegans*, we wanted to determine if the genes with the largest fold change in expression were among the known IIS and Nrf2 regulons. Focusing on genes with a significant absolute LFC>3, we observed that among

the 24 most upregulated genes, 83% (20) have previously been observed to be regulated by the IIS pathway and 71% (17) have been observed to be regulated by the Nrf2 pathway (Supplemental table 1). Interestingly, the four genes without a known connection to the IIS pathway appear non-random. For example, the most upregulated gene (*E02C12.10*, LFC=9.9) is a member of a family of 31 paralogs in *C. elegans* predicted to have kinase-like activity (Davis et al., 2022; Vilella et al., 2009). Interestingly, the *E02C12.10* gene, which clearly merits further investigation, was also identified as a significant contributor to survival of AMPK-deficient dauer larvae using a genome-wide RNAi screen (Xie and Roy, 2012). Two additional members of the "most upregulated" gene set (*E02C12.12* and *E02C12.6*) were also members of this gene family, in addition to 10 additional genes in the upregulated WaRGS, representing 32% of all family members and ~48% (10/21) of the family members detected in our dataset, a significant enrichment over the observed rate (1.3%, $p<0.0001$). In contrast with the upregulated WaRGs, none of the family members were classified as downregulated WaRGs. The function of these genes is unknown, but the family is defined by a putative protein kinase domain and a nuclear hormone receptor like structure (Davis et al., 2022) that suggests a potential for transduction of an atRA regulatory response. There were fewer downregulated genes with an LFC<-3, with only 12 genes reaching the threshold. Among those 12 genes, 100% have previously been shown to be regulated by both the IIS and Nrf2 pathways (Supplemental table 2).

Overall, consistent with our genetic results, there is a clear footprint of atRA activity across a broad set of stress-response and longevity-related pathways, with some indication of novel activity as well.

The HSF-1 transcription factor is an important effector of the overall atRA transcriptional response

To further dissect the transcriptional response to atRA in detail, we repeated our transcriptional analysis in several mutant backgrounds. Using *hsf-1(sy441)* mutants, we were able to identify mRNA from 13,737 genes (compared to 12,746 in N2). A comparison of transcriptional responses to atRA for all genes shows that there is a strong correlation between the N2 and *hsf-1(sy441)* expression changes ($R^2=0.306$, $p<0.0001$) (Figure 6A). Using the same cutoffs that we used for our wildtype dataset to define WaRGs, we determined that the atRA regulon for *hsf-1(sy441)* animals (298/13737) is ~42% the size of wildtype (653/12,746), with half of the response unique to *hsf-1(sy441)* (Figure 6B). Comparing the 653 WaRGs from the general analysis with the subset identified in *hsf-1* mutants, ~96% (629/653) were detected in both datasets. Among the 470 downregulated WaRGs, only 14% (64/470) still meet the WaRG thresholds in the *hsf-1* background. Among the 158 upregulated WaRGs that were detectible in our *hsf-1(sy441)* dataset, half (79/158) of the genes still met the threshold for classification as a WaRG. The loss of differential expression could result from fewer genes changing expression, or by a decrease in magnitude of the response that drops genes below our current threshold for defining WaRG genes. This potential for "lost" regulation would be particularly skewed for genes whose expression change was near the absolute LFC=1 threshold, where a negligible change could alter the categorization of the response. We therefore categorized the WaRG response as being maintained (0.5-2x WT response), weakened (<0.5X WT), lost (FDR>.05), or flipped in the *hsf-1* background (Figure 6C). We found that a greater portion of the downregulated WaRG response was dependent on *hsf-1*, with only 29% of the downregulated response being maintained, compared to 61% of the upregulated response (Figure 6D). We then sought to determine if the lost and maintained WaRGs represented unique functions by performing an enrichment analysis using the WormCat analysis tool (Figure 6 figure supplement 1). We found that the maintained response was enriched for sphingolipid (6/44, $p=6.1e-06$), sterol (6/59, $p=6.9e-04$), and short chain dehydrogenase (6/42, $p=0.00011$) metabolism genes. Additionally, the maintained response was also enriched for C-type lectin (10/256, $p=0.00029$), CYP detoxification (10/82, $p=1.7e-07$), and CUB pathogen (4/25, $p=0.004$) stress response genes. The same analysis of the lost WaRG response genes suggests an *hsf-1* dependence for atRA regulation of solute carrier (12/197, $p= 0.000103$), neuropeptide (10/139, $p= 0.000196$) and stress response genes. Thus, *hsf-1* plays an important, but hardly absolute, role in mediating the atRA longevity response.

Loss of AMPK results in both lost and gained transcriptional responses to atRA

To determine the role of AMPK in regulating the transcriptional response to atRA, we repeated our RNAseq analysis in *aak-2(ok524)* mutants. A comparison of the transcriptional response to atRA for all genes shows that there is a strong correlation between the N2 and *aak-2(ok524)* data sets for expression changes ($R^2=0.589$, $p<0.0001$) (Figure 6E). Using the same cutoffs that we used for our wildtype dataset to define WaRGs, we determined that the atRA regulon for *aak-2(ok524)* mutants (802/12,611) is actually larger than wildtype (653/12,746), with more than half (456/802) of the response unique to *aak-2(524)* (Figure 6F). We next sought to determine what portion of the wildtype atRA transcriptional response was lost in *aak-2* mutants. We therefore analyzed the 96% of the WaRGs (627/653) that were detected in our *aak-2* dataset and found that 76% (122/160) of the upregulated and 79% (367/467)

of the downregulated WaRGs were similarly regulated in *aak-2* animals (Figure 6G,H). A WormCat 2.0 analysis (Figure 6 figure supplement 1) of the maintained atRA response demonstrated enrichment for secreted extracellular proteins (7/54, p=0.004), collagen (12/184, p=.006) and solute carrier (18/197, p=8.67e-7) genes. The maintained response was also enriched for sphingolipid (6/44, p=1.5e-06) metabolism genes, suggesting that this metabolism category of changed expression observed in wildtype animals is upstream of *aak-2*. Additionally, there is an enrichment for caenacin (4/11, p=.007), and CUB pathogen (5/25, p=.009) stress response genes. There was also an enrichment for ABC transmembrane transport (9/50, p= 82.9e-5) and cathepsin (5/22, p=.005) genes. We conclude that while *aak-2* is absolutely required for the longevity effects of atRA, *aak-2* is required for only a small proportion (~1/4) of the transcriptional response.

AAK-2 functions downstream of HSF-1 in the transcriptional response to atRA

Given that HSF-1 and AAK-2 are both required for atRA lifespan extension, we sought to determine if HSF-1 and AAK-2 act in series or in parallel. Because a typical genetic analysis of longevity would not enable such a determination, we turned to the atRA transcriptional response (653 WaRGs) identified in wildtype animals. Compared to our datasets from *aak-2(ok524)* and *hsf-1(sy441)*, 610/653 WaRGs were detectible in both mutants. We therefore analyzed those 610 genes for patterns of transcriptional response. We observed that *aak-2(ok524)* mutants retained a larger portion of the response, with 84.4% (515/610) of the WaRGs still being differentially expressed (FDR<.05) in the *aak-2(ok524)* mutants, while only 52.6% (315/610) were in *hsf-1(sy441)* animals.

We next sought to categorize the atRA response overlap between mutants. We first used our normalized LFCΔ-based classification of WaRGs (maintained, enhance, lost, weakened, or flipped) to determine the relationship between regulation in *hsf-1* and *aak-2* backgrounds. We find that nearly 87% (85/98) of the lost response in *aak-2* was also lost in *hsf-1* animals, while nearly 90% of the response retained in *hsf-1(sy441)* animals was retained in *aak-2(ok524)* animals (208/232; Figure 6 figure supplement 2). These results are inconsistent with two parallel responses where we would expect (mostly) non-overlapping classes of regulated (lost) genes. In fact, we see a significant enrichment of overlap beyond the expected overlap for random regulation between *hsf-1* and *aak-2*. This suggests that HSF-1 and AAK-2 regulators act in series, with *hsf-1* upstream of *aak-2*, in the atRA pathway.

We then reanalyzed the WaRGs after sub-setting based on response in the mutant backgrounds. We found no enrichments at the levels used in our previous analyses for the response lost in both genetic backgrounds. In contrast, we observed enrichments for iron, amino acid, and sphingolipid metabolism among those genes whose response was maintained in both *hsf-1* and *aak-2* backgrounds. We interpret these changes to be either independent of the atRA longevity pathway, or upstream of *hsf-1* in the atRA longevity response. A similar analysis of the 212 WaRGs that were lost in *hsf-1(sy441)*, but retained in *aak-2*, showed an enrichment for fatty acid biosynthesis and UGT pathway genes. Interestingly, HSF1 has been implicated in regulating fatty acid biosynthesis in mammals (Jin et al., 2011), suggesting a potentially conserved *hsf-1* function that lies upstream of *aak-2* in the atRA longevity response.

Discussion

The translation of the biology of aging to improvements in human health will require an extensive and varied set of interventions as candidates for clinical trials. Amongst these interventions, small drug-like chemical compounds, or actual approved drugs, are likely to feature in translation. There is now a 25-year-old history of experiments showing small molecule extension in lifespan in simple laboratory animals and a 15-year history of extending lifespan in laboratory mice. Identifying novel compounds that hold the potential to extend life, especially if they do so by increasing the overall period of healthy living (healthspan) and not just lifespan *per se* (Crimmins, 2015; "Increasing Healthspan," 2015) is of import. While there have been some celebrated successes in this area, the chemical space explored to date for longevity interventions is small. Hence, the field is shifting toward a systematic appraisal of a more comprehensive set of target compounds. One potential method of accomplishing this goal is to use a broad collection of information on biological activity and structural characteristics of individual compounds to create a "training set" that allows computational prediction of compound effects, thereby providing a means of prioritizing validation efforts in the face of many hundreds of thousands of potential options. Here we present a "proof of concept" of this approach using a comprehensive, multi-species approach in *Caenorhabditis* nematodes via the *Caenorhabditis* Intervention Testing Program (CITP) that draws upon a previously published set of compounds predicted to have positive effects on lifespan-related pathways (Fuentealba et al., 2019). Overall, focusing primarily on top ranked and novel compounds, we find the mining of these predictions can be highly effective, with more than 31% of tested compounds leading to an increase in lifespan. When this list is augmented by additional predicted compounds previously tested by the CITP (and therefore

not retested here), the prediction success rate stays very similar at 30% (Table 1). In comparison, several large-scale compound screens in *C. elegans* yielded much lower initial hit rates (<2%) and required multiple rounds of experimental validation to narrow down compounds to move forward into full lifespan assays (Petrascheck, Ye & Buck, 2007; Lucanic et al., 2016). The retest hit rate in both of these studies was less than 0.2%.

While most compounds tested here had relatively moderate effects (<15% increase in median lifespan), two interventions conferred large effects, including propranolol with a greater than 44% increase in median lifespan and all-trans retinoic acid (atRA), with a greater than 23% increase in median lifespan in *C. elegans*. The effects of both compounds were variable and were much reduced in related species *C. briggsae* and *C. tropicalis*, which has been a common feature of CITP tests for reasons that remain currently unknown (Banse et al., 2024c, 2019; Lucanic et al., 2017; Onken et al., 2022). Fortunately, *C. elegans* itself has been a reliable testing platform, including robust responses across a wide set of genetic backgrounds (Banse et al. 2019). Tests of the effect of propranolol directly on bacterial growth suggest that the increase in lifespan with that treatment might be caused by a dietary-restriction like response in the nematodes, since growth of the bacteria that serve as their food source is inhibited under propranolol exposure. This effect deserves further investigation but was outside of the scope of the current project.

Of the sixteen compounds initially targeted, atRA emerged as the most interesting candidate, with positive effects on both lifespan and locomotory healthspan across diverse natural isolates of *C. elegans*. The positive effects of atRA have also been indicated by other studies, which generated a positive hit using a distinct approach involving the maintenance of collagen expression in adult *C. elegans* (Statzer et al., 2021). As such, atRA presented itself as an ideal candidate for using the power of nematode genetics to move from computational prediction to functional analysis. The fact that atRA is already an FDA approved intervention for other indications makes it a particularly inviting compound. This observation is strengthened by the recent observation that the atRA precursor Vitamin A can also enhance longevity in *C. elegans* and does so in a *skn-1* dependent manner (Sirakawin et al. 2023).

Putative atRA targets

Analysis of mutants in a number of key regulatory and stress-response systems treated with atRA suggests that atRA functions through the AKT-1 and AKT-2 kinases to affect conserved AMPK, Nrf2, and HSF1 pathways. Using a comprehensive RNA-seq approach with and without atRA treatment in both wildtype and mutant backgrounds suggests extensive remodeling of sphingolipid and fatty acid metabolic networks, both of which are known to modulate lifespan. While these data support a model for atRA affecting longevity through Akt and its downstream longevity transcription factors *hsf-1* and *skn-1*, the mechanism of initiation upstream of Akt remains unknown. One explanatory model of upstream initiation is suggested by our observation that atRA transcriptionally alters sphingolipid metabolism in *C. elegans*, which has also been seen in mammals (Camdzic et al., 2023; Clarke et al., 2011; Kalén et al., 1992; Sun and Wang, 2021). Sphingolipids are known to regulate developmental rate and lifespan in *C. elegans* (Cutler et al., 2014), and potentially in mammals as well (Cutler and Mattson, 2001). For example, remodeling the sphingolipid metabolism network through RNAi induced reductions in *ttm-5* (dihydroceramide desaturase homologue), *W02F12.2* (neutral/acidic ceramidase homologue), *cgt-2* (glucosylceramide synthase homologue) or *K06A9.1* (neutral sphingomyelinase homolog), all result in lifespan extension. Additionally, genetic disruption of the ceramide synthases alters lifespan, with loss of *hyl-2* shortening and simultaneous loss of *hyl-1* and *lagr-1* extending *C. elegans* lifespan through a *skn-1* dependent process (Mosbech et al., 2013). Additionally, the control of the relative ceramide and sphingomyelin levels by sphingomyelin synthases mediates crosstalk between DAF-16 and CREBH (He et al., 2021), which would have a significant impact on glucose and lipid metabolism, and therefore longevity. As such, the atRA-altered sphingolipid network observed in our RNAseq data (Figure 5B; Figure 5 supplemental figure 2) could have significant impacts on longevity.

The importance of sphingolipid regulation of metabolism, and ultimately lifespan, is not a unique feature of nematodes. The network has been proposed to function in mammals as a metabolic rheostat that uses the ratios of ceramide, ceramide-1P, sphingosine, and sphingosine-1P to determine metabolic regulatory response (Summers et al., 2019). This may be a mechanistic contributor to atRA longevity effects as there is known cross-talk between longevity pathways and ceramide/sphingolipids (Jęśko et al., 2019). Interestingly, ceramide and sphingolipid metabolism may provide a conserved functional connection to the observed relationship between atRA and Protein Kinase B/Akt function. In cell culture, treatment with atRA increases ceramide levels (Kalén et al., 1992), and cell-permeable ceramide inhibits Akt kinase activity (Zhou et al., 1998). Additionally, exogenous ceramide induces dephosphorylation and inhibition of Akt (Zinda et al., 2001). This functionality is known to be biologically relevant, as ceramide is a known negative regulator of insulin activity via regulation of Akt (Hsieh et al., 2014).

Considering these findings, a simple model consistent with our observations is that the application of atRA changes sphingolipid metabolism, which in turn induces a change in the functional state of *akt-1* and *akt-2*. Our observations that HSF-1, AAK-2, and SKN-1 are necessary for atRA longevity extension are easily understood within this model, as all three have been identified as potential direct targets of Akt regulation. How (and if) atRA directly regulates sphingolipid metabolism remains an open question. In cell culture, atRA induces growth arrest in many cell types, and that arrest is mediated through nSMase2 induction, which increases ceramide levels (Clarke et al., 2011). Additionally, the involvement of sphingosine kinases in atRA signaling has been demonstrated in K562 chronic myeloid leukemia cells (Sun and Wang, 2021), but the identity of the transcriptional effector remains unclear.

Conservation of aging effects of atRA

The retinoids—atRA in particular—are broadly conserved regulators of transcription (Amann et al., 2011). In vertebrates, atRA functions in a broad range of biological activities, from development (Duester, 2008; Niederreither and Dollé, 2008), immune function (Huang et al., 2018), and memory and learning, to energy metabolism (Zhang et al., 2015). In mammals, some research suggests a potential role for atRA signaling in modulating aging. Among clinical aging studies of both natural and synthetic retinoids, the bulk of the research has been for aging and/or UV-photoaging of skin. Among those studies, atRA is the most widely investigated retinoid, and potentially the most potent (Mukherjee et al., 2006). Beyond skin phenotypes, studies in mouse models have also shown that age-dependent decreases in atRA signaling result in poor performance on spatial learning and memory tasks, and dietary supplementation with atRA can ameliorate the age-related decreases in hippocampal long-term-memory potentiation and other brain functions (Etchamendy et al., 2001). The potential use of atRA as an intervention in age-related diseases of neurophysiology has not been ignored and is receiving significant attention as a therapeutic for Alzheimer's Disease and related dementias (Das et al., 2019; H.-P. Lee et al., 2009; Szutowicz et al., 2015).

While atRA may function as an anti-aging agent due to the phenotypic outcomes of application, the molecular mechanisms responsible for these activities are not fully understood. One possibility is that atRA functions as a high affinity ligand for PPARβ/δ peroxisome proliferation-activated receptor, which is a master regulator of lipid metabolism and glucose homeostasis. Activation of PPARβ/δ increases lipid catabolism in adipose tissue and skeletal muscle to prevent obesity (Kuri-Harcuch, 1982; Pairault et al., 1988; Sato et al., 1980; Schwarz et al., 1997). Additionally, in an obese mouse model, treatment with atRA induced PPARβ/δ and RAR regulated genes, correlating with weight loss and improved insulin responsiveness (Berry and Noy, 2009). Alternatively, atRA could be affecting longevity through effects on Akt proteins, as we observed and has been shown for other atRA phenotypes in mammals. Indeed, multiple pathways are likely to be engaged.

Summary

We tested the hypothesis that using intersecting computational predictions can identify aging interventions at a high frequency in *Caenorhabditis* species. We found that using cross-validated computational predictions resulted in a high discovery rate (30%), which is compatible with screening across a dosage range using full lifespan analysis. The future success of computational prediction approaches should increase as AI methodologies are brought to bear on an ever-increasing body of research. In the example described above, computational predictions led to the identification of an endogenous signaling ligand that regulates metabolism and can be co-opted to extend life. Our study demonstrates the potential of metabolic manipulation for aging interventions and the benefits of computational predictions in prioritizing a compound screening.

Materials and Methods

A detailed set of standard operating procedures is available online (*Caenorhabditis* Intervention Testing Program, 2025). The experimental details in brief are as follows:

Caenorhabditis *strains and maintenance*

All *Caenorhabditis* strains were obtained from the *Caenorhabditis* Genetics Center: N2-PD1073 (Teterina et al., 2022; Yoshimura et al., 2019); CF1038 *daf-16(mu86)* (Lin et al., 1997); DA1113 *eat-2(ad1113)* (Raizen et al., 1995); IG10 *tol-1(nr2033)* (Pujol et al., 2001); RB754 *aak-2(ok524)* (*C. elegans* Deletion Mutant Consortium, 2012); PS3551 *hsf-1(sy441)* (Hajdu-Cronin et al., 2004); KU25 *pmk-1(km25)* (Mizuno et al., 2004); RB759 *akt-1(ok525)*; VC204 *akt-2(ok393)*. Wild isolates in this study include *C. elegans* JU775 and MY16, *C. briggsae* AF16, ED3092 and HK104, and *C. tropicalis* JU1630, JU1373, and QG834. All strains were maintained on nematode growth medium (NGM) plates

566 seeded with *Escherichia coli* OP50-1 at 20˚C. For experimental synchronization, cohorts were generated by timed egg-
567 lays (Lucanic et al., 2017).

568 ***Compound treatment***

569 Compound treatment was conducted as previously published (Banse et al., 2019; Lucanic et al., 2017). Compounds
570 were obtained as a solid and dissolved in DMSO (dimethyl sulfoxide) or H_2O to obtain a stock solution. The following
571 compounds were used: temsirolimus (Cayman 11590), ritonavir (Simga-Aldrich SML0491), thalidomide (Calbiochem
572 585970), arecoline (Cayman 13662), everolimus (Caymen 11597), temsirolimus (Cayman 11590), erlotinib (Cayman
573 10483), berberine (Cayman 10006427), dasatinib (Cayman 11498), propranolol (Sigma-Aldrich P0884), aldosterone
574 (Sigma-Aldrich A9477), dexamethasone (Sigma-Aldrich D1756), gefitinib (Sigma-Aldrich SML1657), tretinoin (all-
575 trans retinoic acid) (Sigma-Aldrich PHR1187), bortezomib (Sigma-Aldrich 5043140001), decitabine (Selleck Chemical
576 S1200), fisetin (Tocris 5016), and metoprolol (Sigma-Aldrich M5391). DMSO stock solutions were mixed with water
577 to form a working solution before being added to plates. In-plate concentrations were calculated by presuming the final
578 volume to be equal to that of the volume of agar. For 50, 100, and 150 µM atRA plates, stock solutions formed
579 precipitates at working solution concentrations, requiring working solutions to be prepared individually for each plate.

580 ***Lifespan assays***

581 Lifespan assays were performed as previously published (Banse et al., 2019; Lucanic et al., 2017). Briefly, worms were
582 age-synchronized via timed egg lays and transferred to control or compound treated plates on days one, two, and five
583 of adulthood (or day four for *C. tropicalis* strains), and once weekly thereafter until dead. All lifespans were conducted
584 using 51 µM FUdR (5-Fluoro-2'-deoxyuridine) to prevent progeny production (Hosono, 1978; Lucanic et al., 2017;
585 Mitchell et al., 1979). For automated lifespan assays, worms were transferred to the Automated Lifespan Machines
586 (Epson Perfection V800s) (Abbott et al., 2020) on day five (*C. elegans* and *C. briggsae*) or day four (*C. tropicalis*) of
587 adulthood, at which point survival data was collected and analyzed using the Lifespan Machine software
588 (https://github.com/nstroustrup/ lifespan (Stroustrup et al., 2013)). For lifespans using RNAi feeding, RNAi plates
589 (25 mg/L carbenicillin and 1 mM IPTG) were seeded using an RNase II deficient *E. coli* strain (HT115) harboring either
590 the *skn-1* (T19E7.2) targeting or control L4440 plasmid from the Ahringer RNAi library (Kamath and Ahringer, 2003).
591 Worms were transferred to RNAi plates at the L3/L4 stage before being transferred to compound treated RNAi plates
592 containing 51 µM FUdR on day one of adulthood. An additional transfer on day three of adulthood was also added for
593 lifespans using RNAi. All lifespan assays were conducted at 20˚C and 80% relative humidity with 50 animals per pertri
594 plate. Analysis of propranolol effects in the presence of paraformaldehyde treated bacteria was performed as published
595 (Beydoun et al., 2023).

596 ***CeleST health assays***

597 *CeleST* health assays were performed as previously published (Banse et al., 2024b). In brief, animals were exposed to
598 compound intervention during adulthood as described above until CeleST measurements were collected at two
599 timepoints (adult days 6 and 12 for *C. elegans* and *C. tropicalis*, and days 8 and 16 for *C. briggsae*). For two biological
600 replicates at each of the three CITP sites, 40 animals were tested per condition (age and compound or control) per strain.
601 For full experimental protocols see our online protocol (*Caenorhabditis* Intervention Testing Program, 2022). Eight
602 different parameters (Wave initiation rate, Body wave number, Asymmetry, Stretch, Curling, Travel speed, Brush
603 stroke, and Activity index (Ibáñez-Ventoso et al., 2016; Restif et al., 2014)) were measured using the CeleST software
604 and used to create a composite swimming score (Banse et al., 2024b).

605 ***Statistical analysis***

606 Statistical analyses for lifespan experiments were performed as previously described (Lucanic et al., 2017). In summary,
607 we used a mixed-model approach where compound treatment was considered a fixed effect, and other potential variables
608 were treated as random effects. Survival was analyzed both with generalized linear models using the lme4 (version
609 1.1.32) package (Bates et al., 2015), and a mixed-model Cox-Proportional Hazards (CPH) model using the coxme
610 package (version 2.2-18.1) (Therneau, 2020) in the R statistical language (R Core Team, 2021). The effect of compound
611 treatment was tested using CPH analysis within each strain to allow for each compound treatment replicate to be
612 compared to its specific control in the randomized blocks design. Compound effects were analyzed as a planned
613 comparison between the responses of individuals on the treatment in question and those on the appropriate treatment
614 control. Hits were classified based on a significant *p*-value from the CPH model coupled with an increase in median

lifespan. It should be noted that one compound, aldosterone at 50 µM, showed a significant decrease in the hazard estimate without an increase in median lifespan, and thus was not considered a hit.

Swimming behavior was analyzed using the composite score (described above) as the variable of interest in mixed effects general linear models built for each strain in R using the lme4 package (version 1.1.32) (Bates et al., 2015) as previously described (Banse et al., 2024b). Determination of significant age by compound interactions was made using the R car package (version 3.1-2) (Fox and Weisberg, 2019).

Transcriptomic analysis

For RNA-sequencing, worms were synchronized and compound treated as described above. Four biological replicates of both atRA-treated (150 µM) and vehicle control worms were aged to day four of adulthood and collected in tandem (approximately 50 worms total per replicate). We selected this timepoint because it corresponded to the timepoint at which the Ewald study detected increased *col-144p::GFP* that predicted longevity (Statzer et al., 2021). Worms were picked into 0.2 mL tubes each containing 50 µL of lysis buffer (45 µL elution buffer plus 5 µL proteinase K) and flash frozen with liquid nitrogen, then stored at -80°C until library prep. Libraries were prepared using the KAPA mRNA HyperPrep kit (KK8580 from Kapa Biosystems) as per manufacture protocol except that the total volume was adjusted to ¼ per reaction. Final libraries were normalized by concentration and sequenced on an Illumina Novaseq 6000 with the SP 100 cycle (GC3F, University of Oregon).

Paired-end FASTQ files for all atRA treated and DMSO control samples were aligned to the *C. elegans* WBcel235 (build 104) reference genome using the Subread package (version 2.0.2) (Liao et al., 2013). Uniquely mapped reads were assigned to *C. elegans* genes with Subread's featureCounts program (Liao et al., 2014) using reversely stranded read counting. Subsequent filtering, normalization, and differential expression analysis were performed on each strain-specific dataset with the edgeR package (version 3.28.1) (Robinson et al., 2010), using R (version 3.6.2) (R Core Team, 2021). Lowly expressed genes were removed from each dataset; only genes that had at least 10 reads in at least four samples and a minimum total count of 15 reads across samples were retained. To remove composition biases between libraries, the library sizes were normalized using a trimmed mean of M-values (TMM) (Robinson and Oshlack, 2010) between each pair of samples. A pairwise expression analysis was performed on the transcriptomes of the treatment and control samples from each strain. Quasi-likelihood (QL) F-tests for treatment vs. control sample effect were carried out on fitted gene-wise negative binomial generalized log-linear models. P-values were corrected for false discovery using the Benjamini-Hochberg method.

Data availability

All data is available at citpaging.org/portal. Additionally, transcriptomic data have been deposited in NCBI's Gene are accessible through the NCBI GEO database via accession number GSE272535 (https://www.ncbi.nlm.nih.gov/geo/query/acc.cgi?acc=GSE272535).

Acknowledgements

We acknowledge and thank Max Guo (NIA), Viviana Perez (previously at NIA), Tiziana Cogliati (NIA), and the members of the Phillips, Driscoll, and Lithgow labs for helpful discussions and the Barber lab (University of Oregon) for kindly providing equipment access and technical expertise. Some strains were provided by the CGC, which is funded by NIH Office of Research Infrastructure Programs (P40 OD010440). Some deletion mutants used in this work were generated by the International *C. elegans* Gene Knockout Consortium (*C. elegans* Gene Knockout Facility at the Oklahoma Medical Research Foundation, which is funded by the National Institutes of Health; and the *C. elegans* Reverse Genetics Core Facility at the University of British Columbia, which is funded by the Canadian Institute for Health Research, Genome Canada, Genome B.C., the Michael Smith Foundation, and the National Institutes of Health). This work was directly supported by funding from National Institutes of Health grants (U01 AG045844, U01 AG045864, U01 AG045829, U24 AG056052).

References

Abbott M, Banse SA, Melentijevic I, Jarrett CM, Ange JS, Sedore CA, Falkowski R, Blue BW, Coleman-Hulbert AL, Johnson E, Guo M, Lithgow GJ, Phillips PC, Driscoll M. 2020. A simplified design for the *C. elegans* lifespan machine. *Journal of biological methods* **7**:e137. doi:10.14440/jbm.2020.332

Alavez S, Vantipalli MC, Zucker DJS, Klang IM, Lithgow GJ. 2011. Amyloid-binding compounds maintain protein homeostasis during ageing and extend lifespan. *Nature* **472**:226–9. doi:10.1038/nature09873

Albalat R. 2009. The retinoic acid machinery in invertebrates: ancestral elements and vertebrate innovations. *Mol Cell Endocrinol* **313**:23–35. doi:10.1016/j.mce.2009.08.029

Albalat R, Cañestro C. 2009. Identification of Aldh1a, Cyp26 and RAR orthologs in protostomes pushes back the retinoic acid genetic machinery in evolutionary time to the bilaterian ancestor. *Chem Biol Interact* **178**:188–196. doi:10.1016/j.cbi.2008.09.017

Ali ES, Mitra K, Akter S, Ramproshad S, Mondal B, Khan IN, Islam MT, Sharifi-Rad J, Calina D, Cho WC. 2022. Recent advances and limitations of mTOR inhibitors in the treatment of cancer. *Cancer Cell Int* **22**:284. doi:10.1186/s12935-022-02706-8

AlOkda A, Van Raamsdonk JM. 2022. Effect of DMSO on lifespan and physiology in *C. elegans* : Implications for use of DMSO as a solvent for compound delivery. *MicroPubl Biol* **2022**. doi:10.17912/micropub.biology.000634

Alsayed Y, Uddin S, Mahmud N, Lekmine F, Kalvakolanu DV, Minucci S, Bokoch G, Platanias LC. 2001. Activation of Rac1 and the p38 mitogen-activated protein kinase pathway in response to all-trans-retinoic acid. *J Biol Chem* **276**:4012–4019. doi:10.1074/jbc.M007431200

Amann PM, Eichmüller SB, Schmidt J, Bazhin AV. 2011. Regulation of gene expression by retinoids. *Curr Med Chem* **18**:1405–1412. doi:10.2174/092986711795029618

Amrit FRG, Steenkiste EM, Ratnappan R, Chen S-W, McClendon TB, Kostka D, Yanowitz J, Olsen CP, Ghazi A. 2016. DAF-16 and TCER-1 Facilitate Adaptation to Germline Loss by Restoring Lipid Homeostasis and Repressing Reproductive Physiology in *C. elegans*. *PLoS Genet* **12**:e1005788. doi:10.1371/journal.pgen.1005788

Apfeld J, O'Connor G, McDonagh T, DiStefano PS, Curtis R. 2004. The AMP-activated protein kinase AAK-2 links energy levels and insulin-like signals to lifespan in *C. elegans*. *Genes & development* **18**:3004–9. doi:10.1101/gad.1255404

Austad SN. 2016. The Geroscience Hypothesis: Is It Possible to Change the Rate of Aging? In: Sierra F, Kohanski R, editors. Advances in Geroscience. Cham: Springer International Publishing. pp. 1–36. doi:10.1007/978-3-319-23246-1_1

Avery L. 1993. The Genetics of Feeding in *Caenorhabditis elegans*. *Genetics* **917**:897–917.

Banse SA, Jackson EG, Sedore CA, Onken B, Hall D, Coleman-Hulbert A, Huynh P, Garrett T, Johnson E, Harinath G, Inman D, Guo S, Morshead M, Xue J, Falkowski R, Chen E, Herrera C, Kirsch AJ, Perez VI, Guo M, Lithgow GJ, Driscoll M, Phillips PC. 2024. The coupling between healthspan and lifespan in *Caenorhabditis* depends on complex interactions between compound intervention and genetic background. *Aging (Albany NY)* **16**:5829–5855. doi:10.18632/aging.205743

Banse SA, Lucanic M, Sedore CA, Coleman-Hulbert AL, Plummer WT, Chen E, Kish JL, Hall D, Onken B, Presley MP, Jones EG, Blue BW, Garrett T, Abbott M, Xue J, Guo S, Johnson E, Foulger AC, Chamoli M, Falkowski R, Melentijevic I, Harinath G, Huynh P, Patel S, Edgar D, Jarrett CM, Guo M, Kapahi P, Lithgow GJ, Driscoll M, Phillips PC. 2019. Automated lifespan determination across *Caenorhabditis* strains and species reveals assay-specific effects of chemical interventions. *GeroScience* **41**:945–960. doi:10.1007/s11357-019-00108-9

Banse SA, Sedore CA, Johnson E, Coleman-Hulbert AL, Onken B, Hall D, Jackson EG, Huynh P, Foulger AC, Guo S, Garrett T, Xue J, Inman D, Morshead ML, Plummer WT, Chen E, Bhaumik D, Chen MK, Harinath G, Chamoli M, Quinn RP, Falkowski R, Edgar D, Schmidt MO, Lucanic M, Guo M, Driscoll M, Lithgow GJ, Phillips PC. 2024c. Antioxidants green tea extract and nordihydroguaiaretic acid confer species and strain-specific lifespan and health effects in *Caenorhabditis nematodes*. *Geroscience* **46**:2239–2251. doi:10.1007/s11357-023-00978-0

Barardo D, Newby D, Thornton D, Ghafourian T, Pedro De Magalhães J, Freitas AA. 2017a. Machine learning for predicting lifespan-extending chemical compounds. *Aging* **9**:1721–1737. doi:10.18632/aging.101264

Barardo D, Thornton D, Thoppil H, Walsh M, Sharifi S, Ferreira S, Anžič A, Fernandes M, Monteiro P, Grum T, Cordeiro R, De-Souza EA, Budovsky A, Araujo N, Gruber J, Petrascheck M, Fraifeld VE, Zhavoronkov A, Moskalev A, de Magalhães JP. 2017b. The DrugAge database of aging-related drugs. *Aging cell* **16**:594–597. doi:10.1111/acel.12585

Bastien J, Plassat J-L, Payrastre B, Rochette-Egly C. 2006. The phosphoinositide 3-kinase/Akt pathway is essential for the retinoic acid-induced differentiation of F9 cells. *Oncogene* **25**:2040–2047. doi:10.1038/sj.onc.1209241

Bates D, Mächler M, Bolker B, Walker S. 2015. Fitting Linear Mixed-Effects Models Using lme4. *Journal of Statistical Software*. doi:10.18637/jss.v067.i01

Ben-Sasson H, Ben-Meir A, Shushan A, Karra L, Rojansky N, Klein BY, Levitzki R, Ben-Bassat H. 2011. All-trans-retinoic acid mediates changes in PI3K and retinoic acid signaling proteins of leiomyomas. *Fertil Steril* **95**:2080–2086. doi:10.1016/j.fertnstert.2011.01.155

Berry DC, Noy N. 2009. All-trans-retinoic acid represses obesity and insulin resistance by activating both peroxisome proliferation-activated receptor beta/delta and retinoic acid receptor. *Mol Cell Biol* **29**:3286–3296. doi:10.1128/MCB.01742-08

Beydoun S, Choi HS, Dela-Cruz G, Kruempel J, Huang S, Bazopoulou D, Miller HA, Schaller ML, Evans CR, Leiser SF. 2021. An alternative food source for metabolism and longevity studies in *Caenorhabditis elegans*. *Commun Biol* **4**:258. doi:10.1038/s42003-021-01764-4

Beydoun S, Kitto ES, Wang E, Huang S, Leiser SF. 2023. Methodology to Metabolically Inactivate Bacteria for *Caenorhabditis elegans* Research. *J Vis Exp*. doi:10.3791/65775

Blackwell TK, Steinbaugh MJ, Hourihan JM, Ewald CY, Isik M. 2015. SKN-1/Nrf, stress responses, and aging in *Caenorhabditis elegans*. *Free Radic Biol Med* **88**:290–301. doi:10.1016/j.freeradbiomed.2015.06.008

Bond MR, Ghosh SK, Wang P, Hanover JA. 2014. Conserved nutrient sensor O-GlcNAc transferase is integral to *C. elegans* pathogen-specific immunity. *PLoS One* **9**:e113231. doi:10.1371/journal.pone.0113231

Bowerman B, Eaton BA, Priess JR. 1992. *skn-1*, a maternally expressed gene required to specify the fate of ventral blastomeres in the early *C. elegans* embryo. *Cell* **68**:1061–1075. doi:10.1016/0092-8674(92)90078-q

C. elegans Deletion Mutant Consortium. 2012. Large-scale screening for targeted knockouts in the *Caenorhabditis elegans* genome. *G3 (Bethesda)* **2**:1415–1425. doi:10.1534/g3.112.003830

Caenorhabditis Intervention Testing Program. 2022. *Caenorhabditis* Intervention Testing Program: Healthspan Protocols. *figshare*. doi:10.6084/m9.figshare.c.5089073

Caenorhabditis Intervention Testing Program. 2025. Caenorhabditis Intervention Testing Program: Data, analysis, and SOPs for the all-trans retinoic acid manuscript. *figshare*. Collection. https://doi.org/10.6084/m9.figshare.c.7350250

Camdzic M, Aga DS, Atilla-Gokcumen GE. 2023. Cellular Lipidome Changes during Retinoic Acid (RA)-Induced Differentiation in SH-SY5Y Cells: A Comprehensive In Vitro Model for Assessing Neurotoxicity of Contaminants. *Environ Health (Wash)* **1**:110–120. doi:10.1021/envhealth.3c00022

Carpenter RL, Paw I, Dewhirst MW, Lo H-W. 2015. Akt phosphorylates and activates HSF-1 independent of heat shock, leading to Slug overexpression and epithelial-mesenchymal transition (EMT) of HER2-overexpressing breast cancer cells. *Oncogene* **34**:546–557. doi:10.1038/onc.2013.582

Chen AJ, Li J, Jannasch A, Mutlu AS, Wang MC, Cheng JX. 2018. Fingerprint Stimulated Raman Scattering Imaging Reveals Retinoid Coupling Lipid Metabolism and Survival. *ChemPhysChem* **19**:2500–2506. doi:10.1002/cphc.201800545

Chen D, Frezza M, Schmitt S, Kanwar J, Dou QP. 2011. Bortezomib as the first proteasome inhibitor anticancer drug: current status and future perspectives. *Curr Cancer Drug Targets* **11**:239–253. doi:10.2174/156800911794519752

Chen D, Li PW-L, Goldstein BA, Cai W, Thomas EL, Chen F, Hubbard AE, Melov S, Kapahi P. 2013. Germline signaling mediates the synergistically prolonged longevity produced by double mutations in *daf-2* and *rsks-1* in *C. elegans*. *Cell Rep* **5**:1600–1610. doi:10.1016/j.celrep.2013.11.018

Chiang WC, Ching TT, Lee HC, Mousigian C, Hsu AL. 2012. HSF-1 regulators DDL-1/2 link insulin-like signaling to heat-shock responses and modulation of longevity. *Cell* **148**:322–334. doi:10.1016/j.cell.2011.12.019

Clarke CJ, Mediwala K, Jenkins RW, Sutton CA, Tholanikunnel BG, Hannun YA. 2011. Neutral sphingomyelinase-2 mediates growth arrest by retinoic acid through modulation of ribosomal S6 kinase. *J Biol Chem* **286**:21565–21576. doi:10.1074/jbc.M110.193375

Coleman-Hulbert AL, Johnson E, Sedore CA, Banse SA, Guo M, Driscoll M, Lithgow GJ, Phillips PC. 2019. *Caenorhabditis* Intervention Testing Program: the tyrosine kinase inhibitor imatinib mesylate does not extend lifespan in nematodes. *microPublication Biology* **2019**. doi:10.17912/micropub.biology.000131

Crimmins EM. 2015. Lifespan and Healthspan: Past, Present, and Promise. *The Gerontologist* **55**:901–11. doi:10.1093/geront/gnv130

Cutler RG, Mattson MP. 2001. Sphingomyelin and ceramide as regulators of development and lifespan. *Mech Ageing Dev* **122**:895–908. doi:10.1016/s0047-6374(01)00246-9

Cutler RG, Thompson KW, Camandola S, Mack KT, Mattson MP. 2014. Sphingolipid metabolism regulates development and lifespan in *Caenorhabditis elegans*. *Mechanisms of Ageing and Development* **143–144**:9–18. doi:10.1016/j.mad.2014.11.002

Da Costa R, De Almeida S, Chevarin M, Hadj-Rabia S, Leclerc-Mercier S, Thauvin-Robinet C, Garrido C, Faivre L, Vabres P, Duplomb L, Jego G. 2020. Neutralization of HSF1 in cells from PIK3CA-related overgrowth spectrum patients blocks abnormal proliferation. *Biochem Biophys Res Commun* **530**:520–526. doi:10.1016/j.bbrc.2020.04.146

Dang Y, An Y, He J, Huang B, Zhu J, Gao M, Zhang S, Wang X, Yang B, Xie Z. 2020. Berberine ameliorates cellular senescence and extends the lifespan of mice via regulating p16 and cyclin protein expression. *Aging Cell* **19**:e13060. doi:10.1111/acel.13060

Das BC, Dasgupta S, Ray SK. 2019. Potential therapeutic roles of retinoids for prevention of neuroinflammation and neurodegeneration in Alzheimer's disease. *Neural Regen Res* **14**:1880–1892. doi:10.4103/1673-5374.259604

Davis P, Zarowiecki M, Arnaboldi V, Becerra A, Cain S, Chan J, Chen WJ, Cho J, da Veiga Beltrame E, Diamantakis S, Gao S, Grigoriadis D, Grove CA, Harris TW, Kishore R, Le T, Lee RYN, Luypaert M, Müller H-M, Nakamura C, Nuin P, Paulini M, Quinton-Tulloch M, Raciti D, Rodgers FH, Russell M, Schindelman G, Singh A, Stickland T, Van Auken K, Wang Q, Williams G, Wright AJ, Yook K, Berriman M, Howe KL, Schedl T, Stein L, Sternberg PW. 2022. WormBase in 2022-data, processes, and tools for analyzing *Caenorhabditis elegans*. *Genetics* **220**:iyac003. doi:10.1093/genetics/iyac003

De Genaro P, Simón MV, Rotstein NP, Politi LE. 2013. Retinoic acid promotes apoptosis and differentiation in photoreceptors by activating the P38 MAP kinase pathway. *Invest Ophthalmol Vis Sci* **54**:3143–3156. doi:10.1167/iovs.12-11049

Delaney CE, Chen AT, Graniel JV, Dumas KJ, Hu PJ. 2017. A histone H4 lysine 20 methyltransferase couples environmental cues to sensory neuron control of developmental plasticity. *Development* **144**:1273–1282. doi:10.1242/dev.145722

Dodd W, Tang L, Lone J-C, Wimberly K, Wu C-W, Consalvo C, Wright JE, Pujol N, Choe KP. 2018. A Damage Sensor Associated with the Cuticle Coordinates Three Core Environmental Stress Responses in *Caenorhabditis elegans*. *Genetics* **208**:1467–1482. doi:10.1534/genetics.118.300827

Duangjan C, Rangsinth P, Gu X, Zhang S, Wink M, Tencomnao T. 2019. *Glochidion zeylanicum* leaf extracts exhibit lifespan extending and oxidative stress resistance properties in *Caenorhabditis elegans* via DAF-16/FoxO and SKN-1/Nrf-2 signaling pathways. *Phytomedicine* **64**:153061. doi:10.1016/j.phymed.2019.153061

Duester G. 2008. Retinoic acid synthesis and signaling during early organogenesis. *Cell* **134**:921–931. doi:10.1016/j.cell.2008.09.002

Etchamendy N, Enderlin V, Marighetto A, Vouimba RM, Pallet V, Jaffard R, Higueret P. 2001. Alleviation of a selective age-related relational memory deficit in mice by pharmacologically induced normalization of brain retinoid signaling. *J Neurosci* **21**:6423–6429. doi:10.1523/JNEUROSCI.21-16-06423.2001

Ewald CY, Landis JN, Porter Abate J, Murphy CT, Blackwell TK. 2015. Dauer-independent insulin/IGF-1-signalling implicates collagen remodelling in longevity. *Nature* **519**:97–101. doi:10.1038/nature14021

Farias EF, Marzan C, Mira-y-Lopez R. 2005. Cellular retinol-binding protein-I inhibits PI3K/Akt signaling through a retinoic acid receptor-dependent mechanism that regulates p85-p110 heterodimerization. *Oncogene* **24**:1598–1606. doi:10.1038/sj.onc.1208347

Fletcher M, Tillman EJ, Butty VL, Levine SS, Kim DH. 2019. Global transcriptional regulation of innate immunity by ATF-7 in *C. elegans*. *PLoS Genet* **15**:e1007830. doi:10.1371/journal.pgen.1007830

Fonseca E, Ruivo R, Borges D, Franco JN, Santos MM, C Castro LF. 2020. Of Retinoids and Organotins: The Evolution of the Retinoid X Receptor in Metazoa. *Biomolecules* **10**:594. doi:10.3390/biom10040594

Fox J, Weisberg S. 2019. An R Companion to Applied Regression, Third Edition, R package. ed. Thousand Oaks, CA: Sage.

Fuentealba M, Dönertaş HM, Williams R, Labbadia J, Thornton JM, Partridge L. 2019. Using the drug-protein interactome to identify anti-ageing compounds for humans. *PLoS computational biology* **15**:e1006639. doi:10.1371/journal.pcbi.1006639

Gao AW, Smith RL, van Weeghel M, Kamble R, Janssens GE, Houtkooper RH. 2018. Identification of key pathways and metabolic fingerprints of longevity in *C. elegans*. *Experimental Gerontology* **113**:128–140. doi:10.1016/j.exger.2018.10.003

García-Regalado A, Vargas M, García-Carrancá A, Aréchaga-Ocampo E, González-De la Rosa CH. 2013. Activation of Akt pathway by transcription-independent mechanisms of retinoic acid promotes survival and invasion in lung cancer cells. *Mol Cancer* **12**:44. doi:10.1186/1476-4598-12-44

Garofalo A, Rowlinson M-C, Amambua NA, Hughes JM, Kelly SM, Price NC, Cooper A, Watson DG, Kennedy MW, Bradley JE. 2003. The FAR protein family of the nematode *Caenorhabditis elegans*. Differential lipid binding properties, structural characteristics, and developmental regulation. *J Biol Chem* **278**:8065–8074. doi:10.1074/jbc.M206278200

Giuli MV, Hanieh PN, Giuliani E, Rinaldi F, Marianecci C, Screpanti I, Checquolo S, Carafa M. 2020. Current Trends in ATRA Delivery for Cancer Therapy. *Pharmaceutics* **12**:707. doi:10.3390/pharmaceutics12080707

Golden TR, Melov S. 2004. Microarray analysis of gene expression with age in individual nematodes. *Aging Cell* **3**:111–124. doi:10.1111/j.1474-9728.2004.00095.x

Gonzalez I, Tripathi G, Carter EJ, Cobb LJ, Salih DAM, Lovett FA, Holding C, Pell JM. 2004. Akt2, a novel functional link between p38 mitogen-activated protein kinase and phosphatidylinositol 3-kinase pathways in myogenesis. *Mol Cell Biol* **24**:3607–3622. doi:10.1128/MCB.24.9.3607-3622.2004

Goyala A, Ewald CY. 2023. CRISPR-activated expression of collagen *col-120* increases lifespan and heat tolerance. *MicroPubl Biol* **2023**. doi:10.17912/micropub.biology.000730

Greer EL, Brunet A. 2009. Different dietary restriction regimens extend lifespan by both independent and overlapping genetic pathways in *C. elegans*. *Aging Cell* **8**:113–127. doi:ACE459 [pii] 10.1111/j.1474-9726.2009.00459.x

Greer EL, Dowlatshahi D, Banko MR, Villen J, Hoang K, Blanchard D, Gygi SP, Brunet A. 2007. An AMPK-FOXO pathway mediates longevity induced by a novel method of dietary restriction in *C. elegans*. *Current biology : CB* **17**:1646–56. doi:10.1016/j.cub.2007.08.047

Hajdu-Cronin YM, Chen WJ, Sternberg PW. 2004. The L-type cyclin CYL-1 and the heat-shock-factor HSF-1 are required for heat-shock-induced protein expression in *Caenorhabditis elegans*. *Genetics* **168**:1937–1949. doi:10.1534/genetics.104.028423

Hamer J, Grandjean T, Melendez L, Sowton GE. 1964. EFFECT OF PROPRANOLOL (INDERAL) IN ANGINA PECTORIS: PRELIMINARY REPORT. *Br Med J* **2**:720–723. doi:10.1136/bmj.2.5411.720

He B, Xu J, Pang S, Tang H. 2021. Phosphatidylcholine mediates the crosstalk between LET-607 and DAF-16 stress response pathways. *PLoS Genet* **17**:e1009573. doi:10.1371/journal.pgen.1009573

Hemphill C, Pylarinou-Sinclair E, Itani O, Scott B, Crowder CM, Van Gilst MR. 2022. *Daf-16* mediated repression of cytosolic ribosomal protein genes facilitates a hypoxia sensitive to hypoxia resistant transformation in long-lived germline mutants. *PLoS Genet* **18**:e1009672. doi:10.1371/journal.pgen.1009672

Hertweck M, Göbel C, Baumeister R. 2004. *C. elegans* SGK-1 is the critical component in the Akt/PKB kinase complex to control stress response and life span. *Dev Cell* **6**:577–588. doi:10.1016/s1534-5807(04)00095-4

Hibshman JD, Doan AE, Moore BT, Kaplan RE, Hung A, Webster AK, Bhatt DP, Chitrakar R, Hirschey MD, Baugh LR. 2017. *daf-16*/FoxO promotes gluconeogenesis and trehalose synthesis during starvation to support survival. *Elife* **6**. doi:10.7554/eLife.30057

Higgins DP, Weisman CM, Lui DS, D'Agostino FA, Walker AK. 2022. Defining characteristics and conservation of poorly annotated genes in *Caenorhabditis elegans* using WormCat 2.0. *Genetics* **221**:iyac085. doi:10.1093/genetics/iyac085

Holdorf AD, Higgins DP, Hart AC, Boag PR, Pazour GJ, Walhout AJM, Walker AK. 2020. WormCat: An online tool for annotation and visualization of *Caenorhabditis elegans* genome-scale data. *Genetics* **214**:279–294. doi:10.1534/genetics.119.302919

Hormi-Carver K, Feagins LA, Spechler SJ, Souza RF. 2007. All trans-retinoic acid induces apoptosis via p38 and caspase pathways in metaplastic Barrett's cells. *Am J Physiol Gastrointest Liver Physiol* **292**:G18-27. doi:10.1152/ajpgi.00237.2006

Hosono R. 1978. Sterilization and growth inhibition of *Caenorhabditis elegans* by 5-fluorodeoxyuridine. *Exp Gerontol* **13**:369–374. doi:10.1016/0531-5565(78)90047-5

Hsieh C-T, Chuang J-H, Yang W-C, Yin Y, Lin Y. 2014. Ceramide inhibits insulin-stimulated Akt phosphorylation through activation of Rheb/mTORC1/S6K signaling in skeletal muscle. *Cell Signal* **26**:1400–1408. doi:10.1016/j.cellsig.2014.03.004

Hsu AL, Murphy CT, Kenyon C. 2003. Regulation of aging and age-related disease by DAF-16 and heat-shock factor. *Science* **300**:1142–1145. doi:10.1126/science.1083701

Huang Z, Liu Y, Qi G, Brand D, Zheng SG. 2018. Role of Vitamin A in the Immune System. *J Clin Med* **7**:258. doi:10.3390/jcm7090258

Ibáñez-Ventoso C, Herrera C, Chen E, Motto D, Driscoll M. 2016. Automated Analysis of *C. elegans* Swim Behavior Using CeleST Software. *Journal of visualized experiments : JoVE* **2016**:1–9. doi:10.3791/54359

Increasing Healthspan: Prosper and Live Long. 2015. . *EBioMedicine* **2**:1559. doi:10.1016/j.ebiom.2015.11.015

Inoue H, Hisamoto N, An JH, Oliveira RP, Nishida E, Blackwell TK, Matsumoto K. 2005. The *C. elegans* p38 MAPK pathway regulates nuclear localization of the transcription factor SKN-1 in oxidative stress response. *Genes Dev* **19**:2278–2283. doi:10.1101/gad.1324805

Ishijima N, Kanki K, Shimizu H, Shiota G. 2015. Activation of AMP-activated protein kinase by retinoic acid sensitizes hepatocellular carcinoma cells to apoptosis induced by sorafenib. *Cancer Sci* **106**:567–575. doi:10.1111/cas.12633

Janssens GE, Lin X-X, Millan-Ariño L, Kavšek A, Sen I, Seinstra RI, Stroustrup N, Nollen EAA, Riedel CG. 2019. Transcriptomics-Based Screening Identifies Pharmacological Inhibition of Hsp90 as a Means to Defer Aging. *Cell Reports* **27**:467-480.e6. doi:10.1016/j.celrep.2019.03.044

Jayarathne S, Ramalingam L, Edwards H, Vanapalli SA, Moustaid-Moussa N. 2020. Tart cherry increases lifespan in *Caenorhabditis elegans* by altering metabolic signaling pathways. *Nutrients* **12**. doi:10.3390/nu12051482

Jęśko H, Stępień A, Lukiw WJ, Strosznajder RP. 2019. The Cross-Talk Between Sphingolipids and Insulin-Like Growth Factor Signaling: Significance for Aging and Neurodegeneration. *Mol Neurobiol* **56**:3501–3521. doi:10.1007/s12035-018-1286-3

Jiang S, Jiang C-P, Cao P, Liu Y-H, Gao C-H, Yi X-X. 2022. Sonneradon A Extends Lifespan of *Caenorhabditis elegans* by Modulating Mitochondrial and IIS Signaling Pathways. *Mar Drugs* **20**:59. doi:10.3390/md20010059

Jin X, Moskophidis D, Mivechi NF. 2011. Heat shock transcription factor 1 is a key determinant of HCC development by regulating hepatic steatosis and metabolic syndrome. *Cell Metab* **14**:91–103. doi:10.1016/j.cmet.2011.03.025

Kalén A, Borchardt RA, Bell RM. 1992. Elevated ceramide levels in GH4C1 cells treated with retinoic acid. *Biochim Biophys Acta* **1125**:90–96. doi:10.1016/0005-2760(92)90160-w

Kaletsky R, Lakhina V, Arey R, Williams A, Landis J, Ashraf J, Murphy CT. 2016. The *C. elegans* adult neuronal IIS/FOXO transcriptome reveals adult phenotype regulators. *Nature* **529**:92–6. doi:10.1038/nature16483

Kamath RS, Ahringer J. 2003. Genome-wide RNAi screening in *Caenorhabditis elegans*. *Methods* **30**:313–321. doi:10.1016/s1046-2023(03)00050-1

Kaplan REW, Chen Y, Moore BT, Jordan JM, Maxwell CS, Schindler AJ, Baugh LR. 2015. *dbl-1*/TGF-β and *daf-12*/NHR Signaling Mediate Cell-Nonautonomous Effects of *daf-16*/FOXO on Starvation-Induced Developmental Arrest. *PLoS Genet* **11**:e1005731. doi:10.1371/journal.pgen.1005731

865 Kaushik N, Rastogi S, Verma S, Pandey D, Halder A, Mukhopadhyay A, Kumar N. 2021. Transcriptome Analysis of Insulin Signaling-
866 Associated Transcription Factors in *C. elegans* Reveal Their Genome-Wide Target Genes Specificity and Complexity. *Int J Mol Sci*
867 **22**:12462. doi:10.3390/ijms222212462
868 Kennedy BK, Berger SL, Brunet A, Campisi J, Cuervo AM, Epel ES, Franceschi C, Lithgow GJ, Morimoto RI, Pessin JE, Rando TA,
869 Richardson A, Schadt EE, Wyss-Coray T, Sierra F. 2014. Geroscience: linking aging to chronic disease. *Cell* **159**:709–713.
870 doi:10.1016/j.cell.2014.10.039
871 Kim SC, Kim YH, Son SW, Moon E-Y, Pyo S, Um SH. 2015. Fisetin induces Sirt1 expression while inhibiting early adipogenesis in 3T3-L1
872 cells. *Biochem Biophys Res Commun* **467**:638–644. doi:10.1016/j.bbrc.2015.10.094
873 Kim S-H, Kim B-K, Park S, Park S-K. 2019. Phosphatidylcholine Extends Lifespan via DAF-16 and Reduces Amyloid-Beta-Induced Toxicity
874 in *Caenorhabditis elegans*. *Oxid Med Cell Longev* **2019**:2860642. doi:10.1155/2019/2860642
875 Knutson AK, Rechtsteiner A, Strome S. 2016. Reevaluation of whether a soma-to-germ-line transformation extends lifespan in *Caenorhabditis*
876 *elegans*. *Proc Natl Acad Sci U S A* **113**:3591–3596. doi:10.1073/pnas.1523402113
877 Kostrouch Z, Kostrouchova M, Rall JE. 1995. Steroid/thyroid hormone receptor genes in *Caenorhabditis elegans*. *Proc Natl Acad Sci U S A*
878 **92**:156–159. doi:10.1073/pnas.92.1.156
879 Kumar S, Egan BM, Kocsisova Z, Schneider DL, Murphy JT, Diwan A, Kornfeld K. 2019. Lifespan Extension in *C. elegans* Caused by
880 Bacterial Colonization of the Intestine and Subsequent Activation of an Innate Immune Response. *Developmental Cell* **49**:100-117.e6.
881 doi:10.1016/j.devcel.2019.03.010
882 Kuri-Harcuch W. 1982. Differentiation of 3T3-F442A cells into adipocytes is inhibited by retinoic acid. *Differentiation* **23**:164–169.
883 doi:10.1111/j.1432-0436.1982.tb01279.x
884 Lakowski B, Hekimi S. 1998. The genetics of caloric restriction in *Caenorhabditis elegans*. *Proceedings of the National Academy of Sciences of*
885 *the United States of America* **95**:13091–6.
886 Lan J, Rollins JA, Zang X, Wu D, Zou L, Wang Z, Ye C, Wu Z, Kapahi P, Rogers AN, Chen D. 2019. Translational Regulation of Non-
887 autonomous Mitochondrial Stress Response Promotes Longevity. *Cell Rep* **28**:1050-1062.e6. doi:10.1016/j.celrep.2019.06.078
888 Lazaro-Pena MI, Ward ZC, Yang S, Strohm A, Merrill AK, Soto CA, Samuelson AV. 2022. HSF-1: Guardian of the Proteome Through
889 Integration of Longevity Signals to the Proteostatic Network. *Front Aging* **3**:861686. doi:10.3389/fragi.2022.861686
890 Lee H-P, Casadesus G, Zhu X, Lee H, Perry G, Smith MA, Gustaw-Rothenberg K, Lerner A. 2009. All-trans retinoic acid as a novel therapeutic
891 strategy for Alzheimer's disease. *Expert Rev Neurother* **9**:1615–1621. doi:10.1586/ern.09.86
892 Lee S-J, Murphy CT, Kenyon C. 2009. Glucose shortens the life span of *C. elegans* by downregulating DAF-16/FOXO activity and aquaporin
893 gene expression. *Cell metabolism* **10**:379–91. doi:10.1016/j.cmet.2009.10.003
894 Lee Y, Lee J-Y, Kim MH. 2014. PI3K/Akt pathway regulates retinoic acid-induced Hox gene expression in F9 cells. *Dev Growth Differ*
895 **56**:518–525. doi:10.1111/dgd.12152
896 Lee YM, Lee JO, Jung J-H, Kim JH, Park S-H, Park JM, Kim E-K, Suh P-G, Kim HS. 2008. Retinoic acid leads to cytoskeletal rearrangement
897 through AMPK-Rac1 and stimulates glucose uptake through AMPK-p38 MAPK in skeletal muscle cells. *J Biol Chem* **283**:33969–
898 33974. doi:10.1074/jbc.M804469200
899 Li ST, Zhao HQ, Zhang P, Liang CY, Zhang YP, Hsu AL, Dong MQ. 2019. DAF-16 stabilizes the aging transcriptome and is activated in mid-
900 aged *Caenorhabditis elegans* to cope with internal stress. *Aging Cell* **18**. doi:10.1111/acel.12896
901 Liao Y, Smyth GK, Shi W. 2014. featureCounts: an efficient general purpose program for assigning sequence reads to genomic features.
902 *Bioinformatics* **30**:923–930. doi:10.1093/bioinformatics/btt656
903 Liao Y, Smyth GK, Shi W. 2013. The Subread aligner: fast, accurate and scalable read mapping by seed-and-vote. *Nucleic acids research*
904 **41**:e108. doi:10.1093/nar/gkt214
905 Liberati NT, Fitzgerald KA, Kim DH, Feinbaum R, Golenbock DT, Ausubel FM. 2004. Requirement for a conserved Toll/interleukin-1
906 resistance domain protein in the *Caenorhabditis elegans* immune response. *Proc Natl Acad Sci U S A* **101**:6593–6598.
907 doi:10.1073/pnas.0308625101
908 Lin K, Dorman JB, Rodan A, Kenyon C. 1997. *daf-16*: An HNF-3/forkhead family member that can function to double the life-span of
909 *Caenorhabditis elegans*. *Science* **278**:1319–1322. doi:10.1126/science.278.5341.1319
910 Lu W-C, Omari R, Ray H, Wang J, Williams I, Jacobs C, Hockaden N, Bochman ML, Carpenter RL. 2022. AKT1 mediates multiple
911 phosphorylation events that functionally promote HSF1 activation. *FEBS J* **289**:3876–3893. doi:10.1111/febs.16375
912 Lucanic M, Plummer WT, Chen E, Harke J, Foulger AC, Onken B, Coleman-Hulbert AL, Dumas KJ, Guo S, Johnson E, Bhaumik D, Xue J,
913 Crist AB, Presley MP, Harinath G, Sedore CA, Chamoli M, Kamat S, Chen MK, Angeli S, Chang C, Willis JH, Edgar D, Royal MA,
914 Chao EA, Patel S, Garrett T, Ibanez-Ventoso C, Hope J, Kish JL, Guo M, Lithgow GJ, Driscoll M, Phillips PC. 2017. Impact of
915 genetic background and experimental reproducibility on identifying chemical compounds with robust longevity effects. *Nature*
916 *Communications* **8**:14256. doi:10.1038/ncomms14256
917 Maduro MF, Meneghini MD, Bowerman B, Broitman-Maduro G, Rothman JH. 2001. Restriction of mesendoderm to a single blastomere by the
918 combined action of SKN-1 and a GSK-3beta homolog is mediated by MED-1 and -2 in *C. elegans*. *Mol Cell* **7**:475–485.
919 doi:10.1016/s1097-2765(01)00195-2
920 Mair W, Morantte I, Rodrigues APC, Manning G, Montminy M, Shaw RJ, Dillin A. 2011. Lifespan extension induced by AMPK and
921 calcineurin is mediated by CRTC-1 and CREB. *Nature* **470**:404–408. doi:10.1038/nature09706
922 Mak HY. 2012. Lipid droplets as fat storage organelles in *Caenorhabditis elegans*: Thematic Review Series: Lipid Droplet Synthesis and
923 Metabolism: from Yeast to Man. *J Lipid Res* **53**:28–33. doi:10.1194/jlr.R021006
924 Mark KA, Dumas KJ, Bhaumik D, Schilling B, Davis S, Oron TR, Sorensen DJ, Lucanic M, Brem RB, Melov S, Ramanathan A, Gibson BW,
925 Lithgow GJ. 2016. Vitamin D Promotes Protein Homeostasis and Longevity via the Stress Response Pathway Genes skn-1, ire-1, and
926 xbp-1. *Cell Rep* **17**:1227–1237. doi:10.1016/j.celrep.2016.09.086
927 Masiá S, Alvarez S, de Lera AR, Barettino D. 2007. Rapid, nongenomic actions of retinoic acid on phosphatidylinositol-3-kinase signaling
928 pathway mediated by the retinoic acid receptor. *Mol Endocrinol* **21**:2391–2402. doi:10.1210/me.2007-0062
929 McCormick M, Chen K, Ramaswamy P, Kenyon C. 2012. New genes that extend *Caenorhabditis elegans*' lifespan in response to reproductive
930 signals. *Aging Cell* **11**:192–202. doi:10.1111/j.1474-9726.2011.00768.x

931 McEwan DL, Feinbaum RL, Stroustrup N, Haas W, Conery AL, Anselmo A, Sadreyev R, Ausubel FM. 2016. Tribbles ortholog NIPI-3 and
932 bZIP transcription factor CEBP-1 regulate a *Caenorhabditis elegans* intestinal immune surveillance pathway. *BMC Biology* **14**:1–17.
933 doi:10.1186/s12915-016-0334-6
934 McKay JP, Raizen DM, Gottschalk A, Schafer WR, Avery L. 2004. *eat-2* and *eat-18* are Required for Nicotinic Neurotransmission in the
935 *Caenorhabditis elegans* Pharynx. *Genetics* **166**:161–169. doi:10.1534/genetics.166.1.161
936 Mitchell DH, Stiles JW, Santelli J, Sanadi DR. 1979. Synchronous growth and aging of *Caenorhabditis elegans* in the presence of
937 fluorodeoxyuridine. *J Gerontol* **34**:28–36. doi:10.1093/geronj/34.1.28
938 Mizuno T, Hisamoto N, Terada T, Kondo T, Adachi M, Nishida E, Kim DH, Ausubel FM, Matsumoto K. 2004. The *Caenorhabditis elegans*
939 MAPK phosphatase VHP-1 mediates a novel JNK-like signaling pathway in stress response. *EMBO J* **23**:2226–2234.
940 doi:10.1038/sj.emboj.7600226
941 Mosbech M-B, Kruse R, Harvald EB, Olsen ASB, Gallego SF, Hannibal-Bach HK, Ejsing CS, Færgeman NJ. 2013. Functional loss of two
942 ceramide synthases elicits autophagy-dependent lifespan extension in *C. elegans*. *PLoS One* **8**:e70087.
943 doi:10.1371/journal.pone.0070087
944 Mukherjee S, Date A, Patravale V, Korting HC, Roeder A, Weindl G. 2006. Retinoids in the treatment of skin aging: an overview of clinical
945 efficacy and safety. *Clin Interv Aging* **1**:327–348. doi:10.2147/ciia.2006.1.4.327
946 Mullaney BC, Ashrafi K. 2009. *C. elegans* fat storage and metabolic regulation. *Biochim Biophys Acta* **1791**:474–478.
947 doi:10.1016/j.bbalip.2008.12.013
948 Murphy CT, Hu PJ. 2013. Insulin/insulin-like growth factor signaling in *C. elegans*. *WormBook* 1–43. doi:10.1895/wormbook.1.164.1
949 Narasimhan SD, Yen K, Tissenbaum HA. 2009. Converging pathways in lifespan regulation. *Curr Biol* **19**:R657-666.
950 doi:10.1016/j.cub.2009.06.013
951 Newell Stamper BL, Cypser JR, Kechris K, Kitzenberg DA, Tedesco PM, Johnson TE. 2018. Movement decline across lifespan of
952 *Caenorhabditis elegans* mutants in the insulin/insulin-like signaling pathway. *Aging Cell* **17**:1–14. doi:10.1111/acel.12704
953 Nguyen TTM, An YJ, Cha JW, Cha JW, Ko YJ, Lee H, Chung CH, Jeon SM, Lee J, Park S. 2020. Real-Time In-Organism NMR Metabolomics
954 Reveals Different Roles of AMP-Activated Protein Kinase Catalytic Subunits. *Analytical Chemistry* **92**:7382–7387.
955 doi:10.1021/acs.analchem.9b05670
956 Nhan JD, Turner CD, Anderson SM, Yen C-A, Dalton HM, Cheesman HK, Ruter DL, Uma Naresh N, Haynes CM, Soukas AA, Pukkila-
957 Worley R, Curran SP. 2019. Redirection of SKN-1 abates the negative metabolic outcomes of a perceived pathogen infection. *Proc*
958 *Natl Acad Sci U S A* **116**:22322–22330. doi:10.1073/pnas.1909666116
959 Niederreither K, Dollé P. 2008. Retinoic acid in development: towards an integrated view. *Nat Rev Genet* **9**:541–553. doi:10.1038/nrg2340
960 Nikoletopoulou V, Kyriakakis E, Tavernarakis N. 2014. Cellular and molecular longevity pathways: the old and the new. *Trends Endocrinol*
961 *Metab* **25**:212–223. doi:10.1016/j.tem.2013.12.003
962 Onken B, Driscoll M. 2010. Metformin induces a dietary restriction-like state and the oxidative stress response to extend *C. elegans* healthspan
963 via AMPK, LKB1, and SKN-1. *PloS one* **5**:e8758. doi:10.1371/journal.pone.0008758
964 Onken B, Sedore CA, Coleman-Hulbert AL, Hall D, Johnson E, Jones EG, Banse SA, Huynh P, Guo S, Xue J, Chen E, Harinath G, Foulger AC,
965 Chao EA, Hope J, Bhaumik D, Plummer T, Inman D, Morshead M, Guo M, Lithgow GJ, Phillips PC, Driscoll M. 2022. Metformin
966 treatment of diverse *Caenorhabditis* species reveals the importance of genetic background in longevity and healthspan extension
967 outcomes. *Aging cell* **21**:e13488. doi:10.1111/acel.13488
968 Pairault J, Quignard-Boulange A, Dugail I, Lasnier F. 1988. Differential effects of retinoic acid upon early and late events in adipose conversion
969 of 3T3 preadipocytes. *Exp Cell Res* **177**:27–36. doi:10.1016/0014-4827(88)90022-5
970 Paradis S, Ruvkun G. 1998. *Caenorhabditis elegans* Akt/PKB transduces insulin receptor-like signals from AGE-1 PI3 kinase to the DAF-16
971 transcription factor. *Genes and Development* **12**:2488–2498. doi:10.1101/gad.12.16.2488
972 Park S-K, Link CD, Johnson TE. 2010. Life-span extension by dietary restriction is mediated by NLP-7 signaling and coelomocyte endocytosis
973 in *C. elegans*. *FASEB J* **24**:383–392. doi:10.1096/fj.09-142984
974 Parkhitko AA, Filine E, Mohr SE, Moskalev A, Perrimon N. 2020. Targeting metabolic pathways for extension of lifespan and healthspan
975 across multiple species. *Ageing Res Rev* **64**:101188. doi:10.1016/j.arr.2020.101188
976 Patel DS, Garza-Garcia A, Nanji M, McElwee JJ, Ackerman D, Driscoll PC, Gems D. 2008. Clustering of genetically defined allele classes in
977 the *Caenorhabditis elegans* DAF-2 insulin/IGF-1 receptor. *Genetics* **178**:931–946. doi:10.1534/genetics.107.070813
978 Paysan-Lafosse T, Blum M, Chuguransky S, Grego T, Pinto BL, Salazar GA, Bileschi ML, Bork P, Bridge A, Colwell L, Gough J, Haft DH,
979 Letunić I, Marchler-Bauer A, Mi H, Natale DA, Orengo CA, Pandurangan AP, Rivoire C, Sigrist CJA, Sillitoe I, Thanki N, Thomas
980 PD, Tosatto SCE, Wu CH, Bateman A. 2023. InterPro in 2022. *Nucleic Acids Res* **51**:D418–D427. doi:10.1093/nar/gkac993
981 Peng Y, Sun Q, Gao R, Park Y. 2019. AAK-2 and SKN-1 Are Involved in Chicoric-Acid-Induced Lifespan Extension in *Caenorhabditis*
982 *elegans*. *Journal of Agricultural and Food Chemistry* **67**:9178–9186. doi:10.1021/acs.jafc.9b00705
983 Penkov S, Raghuraman BK, Erkut C, Oertel J, Galli R, Ackerman EJM, Vorkel D, Verbavatz J-M, Koch E, Fahmy K, Shevchenko A,
984 Kurzchalia TV. 2020. A metabolic switch regulates the transition between growth and diapause in *C. elegans*. *BMC biology* **18**:31.
985 doi:10.1186/s12915-020-0760-3
986 Peterson ND, Icso JD, Salisbury JE, Rodríguez T, Thompson PR, Pukkila-Worley R. 2022. Pathogen infection and cholesterol deficiency
987 activate the *C. elegans* p38 immune pathway through a TIR-1/SARM1 phase transition. *Elife* **11**:e74206. doi:10.7554/eLife.74206
988 Petrascheck M, Ye X, Buck LB. 2007. An antidepressant that extends lifespan in adult *Caenorhabditis elegans*. *Nature* **450**:553–6.
989 doi:10.1038/nature05991
990 Prichard BN, Gillam PM. 1964. USE OF PROPRANOLOL (INDERAL) IN TREATMENT OF HYPERTENSION. *Br Med J* **2**:725–727.
991 doi:10.1136/bmj.2.5411.725
992 Pujol N, Link EM, Liu LX, Kurz CL, Alloing G, Tan MW, Ray KP, Solari R, Johnson CD, Ewbank JJ. 2001. A reverse genetic analysis of
993 components of the Toll signaling pathway in *Caenorhabditis elegans*. *Curr Biol* **11**:809–821. doi:10.1016/s0960-9822(01)00241-x
994 Qiao J, Paul P, Lee S, Qiao L, Josifi E, Tiao JR, Chung DH. 2012. PI3K/AKT and ERK regulate retinoic acid-induced neuroblastoma cellular
995 differentiation. *Biochem Biophys Res Commun* **424**:421–426. doi:10.1016/j.bbrc.2012.06.125

R Core Team. 2021. R: A language and environment for statistical computing. R Foundation for Statistical Computing, Vienna, Austria. URL https://www.R-project.org/.

Raizen DM, Lee RY, Avery L. 1995. Interacting genes required for pharyngeal excitation by motor neuron MC in *Caenorhabditis elegans*. *Genetics* **141**:1365–82.

Restif C, Ibáñez-Ventoso C, Vora MM, Guo S, Metaxas D, Driscoll M. 2014. CeleST: computer vision software for quantitative analysis of *C. elegans* swim behavior reveals novel features of locomotion. *PLoS computational biology* **10**:e1003702. doi:10.1371/journal.pcbi.1003702

Ribeiro C, Farmer CK, de Magalhães JP, Freitas AA. 2023. Predicting lifespan-extending chemical compounds for *C. elegans* with machine learning and biologically interpretable features. *Aging (Albany NY)* **15**:6073–6099. doi:10.18632/aging.204866

Robinson MD, McCarthy DJ, Smyth GK. 2010. edgeR: a Bioconductor package for differential expression analysis of digital gene expression data. *Bioinformatics (Oxford, England)* **26**:139–40. doi:10.1093/bioinformatics/btp616

Robinson MD, Oshlack A. 2010. A scaling normalization method for differential expression analysis of RNA-seq data. *Genome Biol* **11**:R25. doi:10.1186/gb-2010-11-3-r25

Roe MM, Hashimi M, Swain S, Woo KM, Bimczok D. 2020. p38 MAPK signaling mediates retinoic acid-induced CD103 expression in human dendritic cells. *Immunology* **161**:230–244. doi:10.1111/imm.13246

Rowlands DJ, Howitt G, Markman P. 1965. PROPRANOLOL (INDERAL) IN DISTURBANCES OF CARDIAC RHYTHM. *Br Med J* **1**:891–894. doi:10.1136/bmj.1.5439.891

Sato M, Hiragun A, Mitsui H. 1980. Preadipocytes possess cellular retinoid binding proteins and their differentiation is inhibited by retinoids. *Biochem Biophys Res Commun* **95**:1839–1845. doi:10.1016/s0006-291x(80)80113-6

Schwarz EJ, Reginato MJ, Shao D, Krakow SL, Lazar MA. 1997. Retinoic acid blocks adipogenesis by inhibiting C/EBPbeta-mediated transcription. *Mol Cell Biol* **17**:1552–1561. doi:10.1128/MCB.17.3.1552

Senchuk MM, Dues DJ, Schaar CE, Johnson BK, Madaj ZB, Bowman MJ, Winn ME, Van Raamsdonk JM. 2018. Activation of DAF-16/FOXO by reactive oxygen species contributes to longevity in long-lived mitochondrial mutants in *Caenorhabditis elegans*. *PLoS Genetics* **14**:1–27. doi:10.1371/journal.pgen.1007268

Seo HW, Cheon SM, Lee M-H, Kim HJ, Jeon H, Cha DS. 2015. Catalpol Modulates Lifespan via DAF-16/FOXO and SKN-1/Nrf2 Activation in *Caenorhabditis elegans*. *Evid Based Complement Alternat Med* **2015**:524878. doi:10.1155/2015/524878

Seo M, Seo K, Hwang W, Koo HJ, Hahm JH, Yang JS, Han SK, Hwang D, Kim S, Jang SK, Lee Y, Nam HG, Lee SJV. 2015. RNA helicase HEL-1 promotes longevity by specifically activating DAF-16/FOXO transcription factor signaling in *Caenorhabditis elegans*. *Proceedings of the National Academy of Sciences of the United States of America* **112**:E4246–E4255. doi:10.1073/pnas.1505451112

Shinozaki Y, Sato Y, Koizumi S, Ohno Y, Nagao T, Inoue K. 2007. Retinoic acids acting through retinoid receptors protect hippocampal neurons from oxygen-glucose deprivation-mediated cell death by inhibition of c-jun-N-terminal kinase and p38 mitogen-activated protein kinase. *Neuroscience* **147**:153–163. doi:10.1016/j.neuroscience.2007.04.032

Sirakawin C, Lin D, Ziyue Z, Xiaoxin W, Kelleher R, Huang S, Long W, Pires-daSilva A, Liu Y, Wang J, Vinnikov IA. 2023. SKN-1/NRF2 upregulation by vitamin A is conserved from nematodes to mammals and is critical for lifespan extension in *Caenorhabditis elegans*. Aging Cell 23:e14064.

Son HG, Seo K, Seo M, Park S, Ham S, An SWA, Choi E-S, Lee Y, Baek H, Kim E, Ryu Y, Ha CM, Hsu A-L, Roh T-Y, Jang SK, Lee S-JV. 2018. Prefoldin 6 mediates longevity response from heat shock factor 1 to FOXO in *C. elegans*. *Genes Dev* **32**:1562–1575. doi:10.1101/gad.317362.118

Sonoda S, Ohta A, Maruo A, Ujisawa T, Kuhara A. 2016. Sperm Affects Head Sensory Neuron in Temperature Tolerance of *Caenorhabditis elegans*. *Cell Rep* **16**:56–65. doi:10.1016/j.celrep.2016.05.078

Soukas AA, Kane EA, Carr CE, Melo JA, Ruvkun G. 2009. Rictor/TORC2 regulates fat metabolism, feeding, growth, and life span in *Caenorhabditis elegans*. *Genes Dev* **23**:496–511. doi:10.1101/gad.1775409

Spindler SR, Li R, Dhahbi JM, Yamakawa A, Sauer F. 2012. Novel protein kinase signaling systems regulating lifespan identified by small molecule library screening using *Drosophila*. *PLoS One* **7**:e29782. doi:10.1371/journal.pone.0029782

Srinivasan AV. 2019. Propranolol: A 50-Year Historical Perspective. *Ann Indian Acad Neurol* **22**:21–26. doi:10.4103/aian.AIAN_201_18

Statzer C, Jongsma E, Liu SX, Dakhovnik A, Wandrey F, Mozharovskyi P, Zülli F, Ewald CY. 2021. Youthful and age-related matreotypes predict drugs promoting longevity. *Aging Cell* **20**:e13441. doi:10.1111/acel.13441

Steinbaugh MJ, Narasimhan SD, Robida-Stubbs S, Moronetti Mazzeo LE, Dreyfuss JM, Hourihan JM, Raghavan P, Operaña TN, Esmaillie R, Blackwell TK. 2015. Lipid-mediated regulation of SKN-1/Nrf in response to germ cell absence. *Elife* **4**:e07836. doi:10.7554/eLife.07836

Steinkraus KA, Smith ED, Davis C, Carr D, Pendergrass WR, Sutphin GL, Kennedy BK, Kaeberlein M. 2008. Dietary restriction suppresses proteotoxicity and enhances longevity by an *hsf-1*-dependent mechanism in *Caenorhabditis elegans*. *Aging Cell* **7**:394–404. doi:10.1111/j.1474-9726.2008.00385.x

Stroustrup N, Ulmschneider BE, Nash ZM, López-Moyado IF, Apfeld J, Fontana W. 2013. The *Caenorhabditis elegans* Lifespan Machine. *Nature methods* **10**:665–70. doi:10.1038/nmeth.2475

Stuhr NL, Curran SP. 2020. Bacterial diets differentially alter lifespan and healthspan trajectories in *C. elegans*. *Communications biology* **3**:653. doi:10.1038/s42003-020-01379-1

Summers SA, Chaurasia B, Holland WL. 2019. Metabolic Messengers: ceramides. *Nat Metab* **1**:1051–1058. doi:10.1038/s42255-019-0134-8

Sun D, Wang S. 2021. Sphingosine kinases are involved in the regulation of all-trans retinoic acid sensitivity of K562 chronic myeloid leukemia cells. *Oncol Lett* **22**:581. doi:10.3892/ol.2021.12842

Szutowicz A, Bielarczyk H, Jankowska-Kulawy A, Ronowska A, Pawełczyk T. 2015. Retinoic acid as a therapeutic option in Alzheimer's disease: a focus on cholinergic restoration. *Expert Rev Neurother* **15**:239–249. doi:10.1586/14737175.2015.1008456

Szymański Ł, Skopek R, Palusińska M, Schenk T, Stengel S, Lewicki S, Kraj L, Kamiński P, Zelent A. 2020. Retinoic Acid and Its Derivatives in Skin. *Cells* **9**:2660. doi:10.3390/cells9122660

1060 Talpaz M, Shah NP, Kantarjian H, Donato N, Nicoll J, Paquette R, Cortes J, O'Brien S, Nicaise C, Bleickardt E, Blackwood-Chirchir MA, Iyer
1061 V, Chen T-T, Huang F, Decillis AP, Sawyers CL. 2006. Dasatinib in imatinib-resistant Philadelphia chromosome-positive leukemias.
1062 *N Engl J Med* **354**:2531–2541. doi:10.1056/NEJMoa055229
1063 Tang L, Choe KP. 2015. Characterization of *skn-1/wdr-23* phenotypes in *Caenorhabditis elegans*; pleiotrophy, aging, glutathione, and
1064 interactions with other longevity pathways. *Mech Ageing Dev* **149**:88–98. doi:10.1016/j.mad.2015.06.001
1065 Tang Z, Su K-H, Xu M, Dai C. 2020. HSF1 physically neutralizes amyloid oligomers to empower overgrowth and bestow neuroprotection. *Sci*
1066 *Adv* **6**:eabc6871. doi:10.1126/sciadv.abc6871
1067 Templeman NM, Luo S, Kaletsky R, Shi C, Ashraf J, Keyes W, Murphy CT. 2018. Insulin Signaling Regulates Oocyte Quality Maintenance
1068 with Age via Cathepsin B Activity. *Curr Biol* **28**:753-760.e4. doi:10.1016/j.cub.2018.01.052
1069 Tepper RG, Ashraf J, Kaletsky R, Kleemann G, Murphy CT, Bussemaker HJ. 2013. PQM-1 complements DAF-16 as a key transcriptional
1070 regulator of DAF-2-mediated development and longevity. *Cell* **154**:676–690. doi:10.1016/j.cell.2013.07.006
1071 Teterina AA, Coleman-Hulbert AL, Banse SA, Willis JH, Perez VI, Lithgow GJ, Driscoll M, Phillips PC. 2022. Genetic diversity estimates for
1072 the *Caenorhabditis* Intervention Testing Program screening panel. *microPublication biology* **2022**.
1073 doi:10.17912/micropub.biology.000518
1074 Teuscher AC, Jongsma E, Davis MN, Statzer C, Gebauer JM, Naba A, Ewald CY. 2019. The in-silico characterization of the *Caenorhabditis*
1075 *elegans* matrisome and proposal of a novel collagen classification. *Matrix Biology Plus* **1**:100001. doi:10.1016/j.mbplus.2018.11.001
1076 Therneau TM. 2020. coxme: Mixed Effects Cox Models. R package version 2.2.16.
1077 Todorova MN, Savova MS, Mihaylova LV, Georgiev MI. 2023. Icariin Improves Stress Resistance and Extends Lifespan in *Caenorhabditis*
1078 *elegans* through *hsf-1* and *daf-2*-Driven Hormesis. *Int J Mol Sci* **25**:352. doi:10.3390/ijms25010352
1079 Troemel ER, Chu SW, Reinke V, Lee SS, Ausubel FM, Kim DH. 2006. p38 MAPK regulates expression of immune response genes and
1080 contributes to longevity in *C. elegans*. *PLoS Genet* **2**:e183. doi:10.1371/journal.pgen.0020183
1081 Tullet JMA, Green JW, Au C, Benedetto A, Thompson MA, Clark E, Gilliat AF, Young A, Schmeisser K, Gems D. 2017. The SKN-1/Nrf2
1082 transcription factor can protect against oxidative stress and increase lifespan in *C. elegans* by distinct mechanisms. *Aging Cell*
1083 **16**:1191–1194. doi:10.1111/acel.12627
1084 Tullet JMA, Hertweck M, An JH, Baker J, Yun J, Liu S, Oliveira RP, Baumeister R, Blackwell TK. 2009. Direct inhibtion of the longevity
1085 promoting factor SKN-1 by Insulin-like signaling *C. elegans*. *Cell* **132**:1025–1038.
1086 Uno M, Honjoh S, Matsuda M, Hoshikawa H, Kishimoto S, Yamamoto Tomohito, Ebisuya M, Yamamoto Takuya, Matsumoto K, Nishida E.
1087 2013. A fasting-responsive signaling pathway that extends life span in *C. elegans*. *Cell Rep* **3**:79–91. doi:10.1016/j.celrep.2012.12.018
1088 Vanhaelen Q, Lin Y-C, Zhavoronkov A. 2020. The Advent of Generative Chemistry. *ACS Med Chem Lett* **11**:1496–1505.
1089 doi:10.1021/acsmedchemlett.0c00088
1090 Vilella AJ, Severin J, Ureta-Vidal A, Heng L, Durbin R, Birney E. 2009. EnsemblCompara GeneTrees: Complete, duplication-aware
1091 phylogenetic trees in vertebrates. *Genome Res* **19**:327–335. doi:10.1101/gr.073585.107
1092 Walker MD, Giese GE, Holdorf AD, Bhattacharya S, Diot C, García-González AP, Horowitz BB, Lee Y-U, Leland T, Li X, Mirza Z, Na H,
1093 Nanda S, Ponomarova O, Zhang H, Zhang J, Yilmaz LS, Walhout AJM. 2021. WormPaths: *Caenorhabditis elegans* metabolic
1094 pathway annotation and visualization. *Genetics* **219**:iyab089. doi:10.1093/genetics/iyab089
1095 Wang X, Zhang J, Lu L, Zhou L. 2015. The longevity effect of echinacoside in *Caenorhabditis elegans* mediated through *daf-16*. *Biosci*
1096 *Biotechnol Biochem* **79**:1676–1683. doi:10.1080/09168451.2015.1046364
1097 Wang Xiangming, Wang Xiaoyan, Li L, Wang D. 2010. Lifespan extension in *Caenorhabditis elegans* by DMSO is dependent on *sir-2.1* and
1098 *daf-16*. *Biochemical and Biophysical Research Communications* **400**:613–618. doi:10.1016/j.bbrc.2010.08.113
1099 Wu C-W, Deonarine A, Przybysz A, Strange K, Choe KP. 2016. The Skp1 Homologs SKR-1/2 Are Required for the *Caenorhabditis elegans*
1100 SKN-1 Antioxidant/Detoxification Response Independently of p38 MAPK. *PLoS Genet* **12**:e1006361.
1101 doi:10.1371/journal.pgen.1006361
1102 Wu Z, Isik M, Moroz N, Steinbaugh MJ, Zhang P, Blackwell TK. 2019. Dietary Restriction Extends Lifespan through Metabolic Regulation of
1103 Innate Immunity. *Cell Metab* **29**:1192-1205.e8. doi:10.1016/j.cmet.2019.02.013
1104 Xie M, Roy R. 2012. Increased levels of hydrogen peroxide induce a HIF-1-dependent modification of lipid metabolism in AMPK compromised
1105 *C. elegans* dauer larvae. *Cell Metab* **16**:322–335. doi:10.1016/j.cmet.2012.07.016
1106 Yilmaz LS, Walhout AJM. 2016. A *Caenorhabditis elegans* Genome-Scale Metabolic Network Model. *Cell Syst* **2**:297–311.
1107 doi:10.1016/j.cels.2016.04.012
1108 Yoshimura J, Ichikawa K, Shoura MJ, Artiles KL, Gabdank I, Wahba L, Smith CL, Edgley ML, Rougvie AE, Fire AZ, Morishita S, Schwarz
1109 EM. 2019. Recompleting the *Caenorhabditis elegans* genome. *Genome research* **29**:1009–1022. doi:10.1101/gr.244830.118
1110 Yousefzadeh MJ, Zhu Y, McGowan SJ, Angelini L, Fuhrmann-Stroissnigg H, Xu M, Ling YY, Melos KI, Pirtskhalava T, Inman CL,
1111 McGuckian C, Wade EA, Kato JI, Grassi D, Wentworth M, Burd CE, Arriaga EA, Ladiges WL, Tchkonia T, Kirkland JL, Robbins
1112 PD, Niedernhofer LJ. 2018. Fisetin is a senotherapeutic that extends health and lifespan. *EBioMedicine* **36**:18–28.
1113 doi:10.1016/j.ebiom.2018.09.015
1114 Yu M, Ge C, Zeng W, Mi Y, Zhang C. 2012. Retinoic acid promotes proliferation of chicken primordial germ cells via activation of PI3K/Akt-
1115 mediated NF-κB signalling cascade. *Cell Biol Int* **36**:705–712. doi:10.1042/CBI20110542
1116 Zacharias FJ, Cowen KJ, Prestt J, Vickers J, Wall BG. 1972. Propranolol in hypertension: a study of long-term therapy, 1964-1970. *Am Heart J*
1117 **83**:755–761. doi:10.1016/0002-8703(72)90206-2
1118 Zhang J, Deng B, Jiang X, Cai M, Liu N, Zhang S, Tan Y, Huang G, Jin W, Liu B, Liu S. 2019. All-Trans-Retinoic Acid Suppresses Neointimal
1119 Hyperplasia and Inhibits Vascular Smooth Muscle Cell Proliferation and Migration via Activation of AMPK Signaling Pathway.
1120 *Front Pharmacol* **10**:485. doi:10.3389/fphar.2019.00485
1121 Zhang R, Wang Y, Li R, Chen G. 2015. Transcriptional Factors Mediating Retinoic Acid Signals in the Control of Energy Metabolism. *Int J*
1122 *Mol Sci* **16**:14210–14244. doi:10.3390/ijms160614210
1123 Zhao X, Lu L, Qi Y, Li M, Zhou L. 2017. Emodin extends lifespan of *Caenorhabditis elegans* through insulin/IGF-1 signaling pathway
1124 depending on DAF-16 and SIR-2.1. *Biosci Biotechnol Biochem* **81**:1908–1916. doi:10.1080/09168451.2017.1365592

1125 Zhavoronkov A, Mamoshina P, Vanhaelen Q, Scheibye-Knudsen M, Moskalev A, Aliper A. 2019. Artificial intelligence for aging and longevity
1126 research: Recent advances and perspectives. *Ageing Res Rev* **49**:49–66. doi:10.1016/j.arr.2018.11.003
1127 Zhou H, Summers SA, Birnbaum MJ, Pittman RN. 1998. Inhibition of Akt kinase by cell-permeable ceramide and its implications for ceramide-
1128 induced apoptosis. *J Biol Chem* **273**:16568–16575. doi:10.1074/jbc.273.26.16568
1129 Zhou KI, Pincus Z, Slack FJ. 2011. Longevity and stress in *Caenorhabditis elegans*. *Aging* **3**:733–53. doi:10.18632/aging.100367
1130 Zinda MJ, Vlahos CJ, Lai MT. 2001. Ceramide induces the dephosphorylation and inhibition of constitutively activated Akt in PTEN negative
1131 U87mg cells. *Biochem Biophys Res Commun* **280**:1107–1115. doi:10.1006/bbrc.2000.4248
1132

Table 1. CITP tested compounds that meet computational prediction selection criteria of this study

Candidate	Predictions	CITP Publication	Beneficial effect on median survival in *C. elegans* in CITP?	Pathway/Mode of action
Bortezomib	F + B	This study	NP	Proteasome inhibitor (Chen et al., 2011)
Metformin	F + J	(Onken et al., 2022)	41% increase at 70 mM	anti-diabetes
17-Alpha estradiol	F + J	(Banse et al., 2024c)	NP	estrogen receptor agonist
Rapamycin	F + J	(Banse et al., 2024c)	NP	mTOR inhibitor
Aspirin	F + J	(Lucanic et al., 2017)	NP	NSAID
Imatinib	F + J + B	(Coleman-Hulbert et al., 2019)	NP	tyrosine kinase inhibitor
atRA	F + J	This study	29% extension at 150 µM	Collagen formation, activates xenobiotic metabolism
Dasatinib	F + B	This study	NP	tyrosine kinase inhibitor
Temsirolimus	F + B	This study	NP	mTOR inhibitor
Gefitinib	F + B	This study	NP	EGFR inhibitor (tyrosine kinase inhibitor)
Resveratrol	F + J	(Lucanic et al., 2017)	12% extension at 100 µM	Sirtuin activator
Berberine	F + B	This study	16.3% extension at 100 µM	AMPK activator
Decitabine	F + B	This study	NP	nucleic acid synthesis inhibitor
Erlotinib	F + B	This study	NP	EGFR inhibitor (tyrosine kinase inhibitor)
Valproic acid	F + J	(Lucanic et al., 2017)	NP	blocks sodium-gated ion channels, increases GABA
Aldosterone	F + B	This study	Significant at 50 µM due to late life effects, no change in median lifespan	Steroid hormone
Dexamethasone	F + B	This study	NP	Anti-inflammatory corticosteroid
Propranolol	F + J	This study	44% extension at 1 mM *	Beta-blocker
Thalidomide	F + J	This study	NP	TNF-a inhibition
Arecoline	F + J	This study	NP	muscarinic agonist (inhibits pharyngeal pumping)
Ritonavir	F + B	This study	4.1% extension at 20 µM	HIV protease inhibitor: inhibits enzymes that normally metabolize other protease inhibitors (primarily in intestines, liver, etc.)
Fisetin	F + D	This study	11.7% extension at 50 µM	Sirtuin activator
Everolimus	F + D	This study	NP	mTOR inhibitor

*may be an indirect effect. NP = no positive effect detected. F - in the top ten percent of (Fuentealba et al., 2019), B - in the top ten percent of (Barardo et al., 2017a), J - in the top ten percent of (Janssens et al., 2019), and D - a positive listing in DrugAge (Barardo et al., 2017b). Compounds denoted in **bold** were tested by the CITP for this study, while other listed compounds were tested previously by the CITP.

Supplemental Table 1— Genes upregulated with a LFC >3 in response to atRA in wildtype CITP N2

				Putative target of known regulatory pathway	
Gene	**LFC**	**P-value**	**FDR**	**IIS (PI3K/Akt)**	**Nrf2 (p38 MAPK)**
E02C12.10	9.9	4.62E-18	5.89E-14		
C52A10.2 (cest-35.2)	8.1	2.5E-16	7.35E-13	*daf-2* (Gao et al., 2018; Senchuk et al., 2018; Sonoda et al., 2016), *daf-16* (Hibshman et al., 2017; Kaplan et al., 2015)	*pmk-1* (Bond et al., 2014)
irld-14	7.4	2.8E-06	0.000111	*daf-2* (Gao et al., 2018)	
gpa-6	6.5	2.68E-14	4.27E-11		
gba-2	6.1	2.88E-16	7.35E-13	*daf-2* (Knutson et al., 2016; M. Seo et al., 2015)	*skn-1* (Nhan et al., 2019), *pmk-1* (Fletcher et al., 2019)
R05D8.9	5.8	1.05E-11	7.06E-09	*daf-16* (Kaplan et al., 2015; Li et al., 2019)	*skn-1*(Nhan et al., 2019)
cyp-33C2	5.7	4.37E-07	2.67E-05	*daf-2* (Chen et al., 2013; Knutson et al., 2016; Sonoda et al., 2016), *daf-16* (Chen et al., 2013)	
cyp-35A4	5.7	7.74E-17	3.29E-13	*daf-2* (Knutson et al., 2016)	*pmk-1* (Bond et al., 2014; Fletcher et al., 2019)
T16G1.6	5.1	1.1E-14	2.01E-11	*daf-2* (Gao et al., 2018; M. Seo et al., 2015; Son et al., 2018), *daf-16* (Delaney et al., 2017; Hibshman et al., 2017; Kaplan et al., 2015)	*pmk-1* (Fletcher et al., 2019)
E02C12.12	5.1	1.44E-06	6.69E-05		
C40H1.8	4.7	2E-12	1.96E-09	*daf-2* (Senchuk et al., 2018), *daf-16* (Li et al., 2019)	
fil-1	4.4	1.23E-12	1.31E-09	*daf-2* (M. Seo et al., 2015), *daf-16* (Kaplan et al., 2015; McCormick et al., 2012; Wu et al., 2016)	*skn-1* (Dodd et al., 2018; Kaushik et al., 2021; Nhan et al., 2019; Steinbaugh et al., 2015; Wu et al., 2016), *pmk-1* (Fletcher et al., 2019)
E02C12.6	4.3	1.57E-10	6.27E-08		*skn-1* (Kaushik et al., 2021; Steinbaugh et al., 2015)
F15H10.7	4.3	3.68E-08	4.36E-06	*daf-2* (Kaletsky et al., 2016)	*skn-1* (Kaushik et al., 2021), *sek-1* (Wu et al., 2019)
hrg-7	3.6	5.84E-17	3.29E-13	*daf-2* (Knutson et al., 2016; M. Seo et al., 2015; Son et al., 2018), *daf-16* (Delaney et al., 2017; Kaplan et al., 2015; S.-J. Lee et al., 2009; Wu et al., 2016)	*skn-1* (Kaushik et al., 2021)
cyp-13A7	3.5	4.44E-08	4.83E-06	*daf-2* (Gao et al., 2018), *daf-16* (Delaney et al., 2017)	*skn-1* (Kaushik et al., 2021)
clec-227	3.4	1.85E-08	2.66E-06	*daf-2* (Senchuk et al., 2018), *daf-16* (Kaplan et al., 2015; Kaushik et al., 2021)	*skn-1* (Dodd et al., 2018; Kaushik et al., 2021)
stdh-2	3.4	4.35E-08	4.78E-06	*daf-2* (Senchuk et al., 2018), *daf-16* (Delaney et al., 2017; Kaplan et al., 2015)	*skn-1* (Dodd et al., 2018), *pmk-1* (Fletcher et al., 2019)
T16G1.4	3.3	1.69E-11	1.08E-08	*daf-2* (Gao et al., 2018; M. Seo et al., 2015; Sonoda et al., 2016), *daf-16* (Delaney et al., 2017; Kaplan et al., 2015; Kaushik et al., 2021; Li et al., 2019; Uno et al., 2013)	*skn-1* (Nhan et al., 2019)
pgp-9	3.3	5.2E-15	1.11E-11	*daf-2* (Sonoda et al., 2016), *daf-16* (Hibshman et al., 2017; Kaplan et al., 2015)	
pgp-7	3.1	2.48E-11	1.5E-08	*daf-2* (Gao et al., 2018), *daf-16* (Kaplan et al., 2015)	*pmk-1* (Bond et al., 2014)
lbp-8	3.1	5.67E-12	4.52E-09	*daf-2* (Gao et al., 2018; Knutson et al., 2016; Sonoda et al., 2016), *daf-16* (Li et al., 2019)	*skn-1* (Dodd et al., 2018; Steinbaugh et al., 2015)
R193.2	3.1	5.14E-10	1.82E-07	*daf-2* (Knutson et al., 2016; Senchuk et al., 2018; Sonoda et al., 2016), *daf-16* (S.-J. Lee et al., 2009, 2009; Li et al., 2019; Patel et al., 2008; Wu et al., 2016)	*skn-1* (Wu et al., 2016), *sek-1* (Wu et al., 2019)
C32H11.9	3.0	2.17E-07	1.56E-05	*daf-2* (Gao et al., 2018; Knutson et al., 2016; Son et al., 2018), *daf-16* (Tepper et al., 2013)	*skn-1* (Dodd et al., 2018), *pmk-1*(Bond et al., 2014; Fletcher et al., 2019)

Supplemental Table 2 – Genes downregulated with a LFC <-3 in response to atRA in CITP N2

				Putative target of known regulatory pathway	
Gene	**LFC**	**P-value**	**FDR**	**IIS (PI3K/Akt)**	**Nrf2 (p38 MAPK)**
Y68A4A.13	-5.8	3.78E-07	2.39E-05	*daf-2* (Senchuk et al., 2018; M. Seo et al., 2015), *daf-16* (Kaplan et al., 2015; Kaushik et al., 2021; Li et al., 2019)	*skn-1* (Kaushik et al., 2021), *sek-1* (Wu et al., 2019)
scl-20	-4.6	5.32E-09	1.06E-06	*daf-2* (Gao et al., 2018; Senchuk et al., 2018; M. Seo et al., 2015; Sonoda et al., 2016), *daf-16* (Amrit et al., 2016; Tepper et al., 2013)	*skn-1* (Nhan et al., 2019), *sek-1* (Wu et al., 2019)
Y9C9A.16	-4.1	2.62E-08	3.52E-06	*daf-2* (Gao et al., 2018; Knutson et al., 2016; Senchuk et al., 2018; M. Seo et al., 2015; Son et al., 2018; Sonoda et al., 2016), *daf-16* (Delaney et al., 2017)	*sek-1* (Wu et al., 2019)
col-183	-4.0	1.13E-08	1.9E-06	*daf-2* (Gao et al., 2018; Knutson et al., 2016; Senchuk et al., 2018; Son et al., 2018; Sonoda et al., 2016)	*skn-1* (Kaushik et al., 2021), *sek-1* (Wu et al., 2019)
C54C8.12	-4.0	6.67E-06	0.00021	*daf-2* (Templeman et al., 2018)	*sek-1* (Wu et al., 2019)
F54E4.2	-3.9	6.05E-09	1.19E-06	*daf-2* (Gao et al., 2018; Kaletsky et al., 2016; M. Seo et al., 2015)	*skn-1* (Nhan et al., 2019)
dhs-26	-3.9	9.61E-13	1.11E-09	*daf-2* (Gao et al., 2018; Knutson et al., 2016; Senchuk et al., 2018; M. Seo et al., 2015; Son et al., 2018; Sonoda et al., 2016), *daf-16* (Kaushik et al., 2021)	*skn-1* (Nhan et al., 2019)
F42A10.7	-3.6	1.2E-08	1.92E-06	*daf-2* (Golden and Melov, 2004; Knutson et al., 2016; Lan et al., 2019),	*skn-1* (Kaushik et al., 2021)
pho-8	-3.3	2.54E-07	1.78E-05	*daf-2* (Knutson et al., 2016; Senchuk et al., 2018; Son et al., 2018), *daf-16* (Amrit et al., 2016; Tepper et al., 2013)	*skn-1* (Kaushik et al., 2021)
C30G12.2	-3.2	3.73E-12	3.4E-09	*daf-2* (Gao et al., 2018; Knutson et al., 2016; Senchuk et al., 2018; M. Seo et al., 2015), *daf-16* (Hemphill et al., 2022)	*skn-1* (Kaushik et al., 2021), *sek-1* (Wu et al., 2019)
irg-4	-3.2	3.65E-13	4.65E-10	*daf-2* (Gao et al., 2018; Knutson et al., 2016; Senchuk et al., 2018; M. Seo et al., 2015; Son et al., 2018; Templeman et al., 2018), *daf-16* (Kaushik et al., 2021; S.-J. Lee et al., 2009; Patel et al., 2008)	*skn-1* (Dodd et al., 2018; Kaushik et al., 2021), *pmk-1* (Bond et al., 2014; McEwan et al., 2016; Troemel et al., 2006)
ftn-1	-3.2	6.58E-11	3.35E-08	*daf-2* (Knutson et al., 2016; Senchuk et al., 2018; M. Seo et al., 2015; Sonoda et al., 2016), *daf-16* (Kaplan et al., 2015)	*skn-1* (Kaushik et al., 2021; Nhan et al., 2019), *sek-1* (Wu et al., 2019)

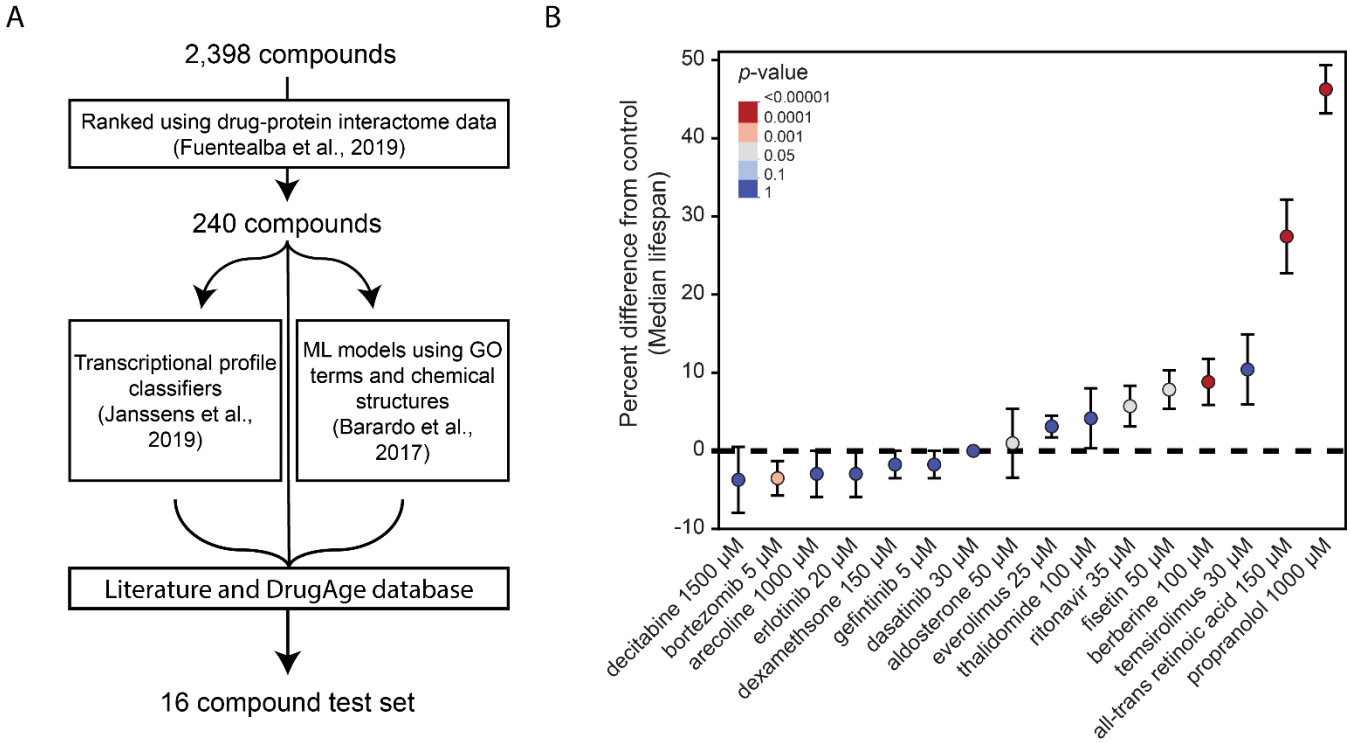

Figure 1. Summary of lifespan effects for candidate compounds. (A) Compounds were selected for testing by filtering the top 10% of predicted hits from (Fuentealba et al., 2019) and cross referencing for compounds that also appeared in the top 10% of (Barardo et al., 2017a), or (Janssens et al., 2019), or had been shown to work in other model organisms via the DrugAge database. Candidate compounds were then filtered using the DrugAge database and a literature search to deprioritize compounds previously characterized as extending lifespan in *C. elegans* to generate a list of 16 compounds for screening using lifespan analysis. (B) Percent difference in median lifespan of individual trial plates compared to the median survival from their pooled carrier control (DMSO and H_2O) for animals treated with one of 16 candidate compounds selected for preliminary analysis. The dot represents the mean of all plate replicates across two trials and the bars represent the standard error. Shown are the results from the longest-lived concentration treatment (4-5 concentrations were tested) for each candidate compound. The shown *p*-values are taken from the CPH model (see materials and methods).

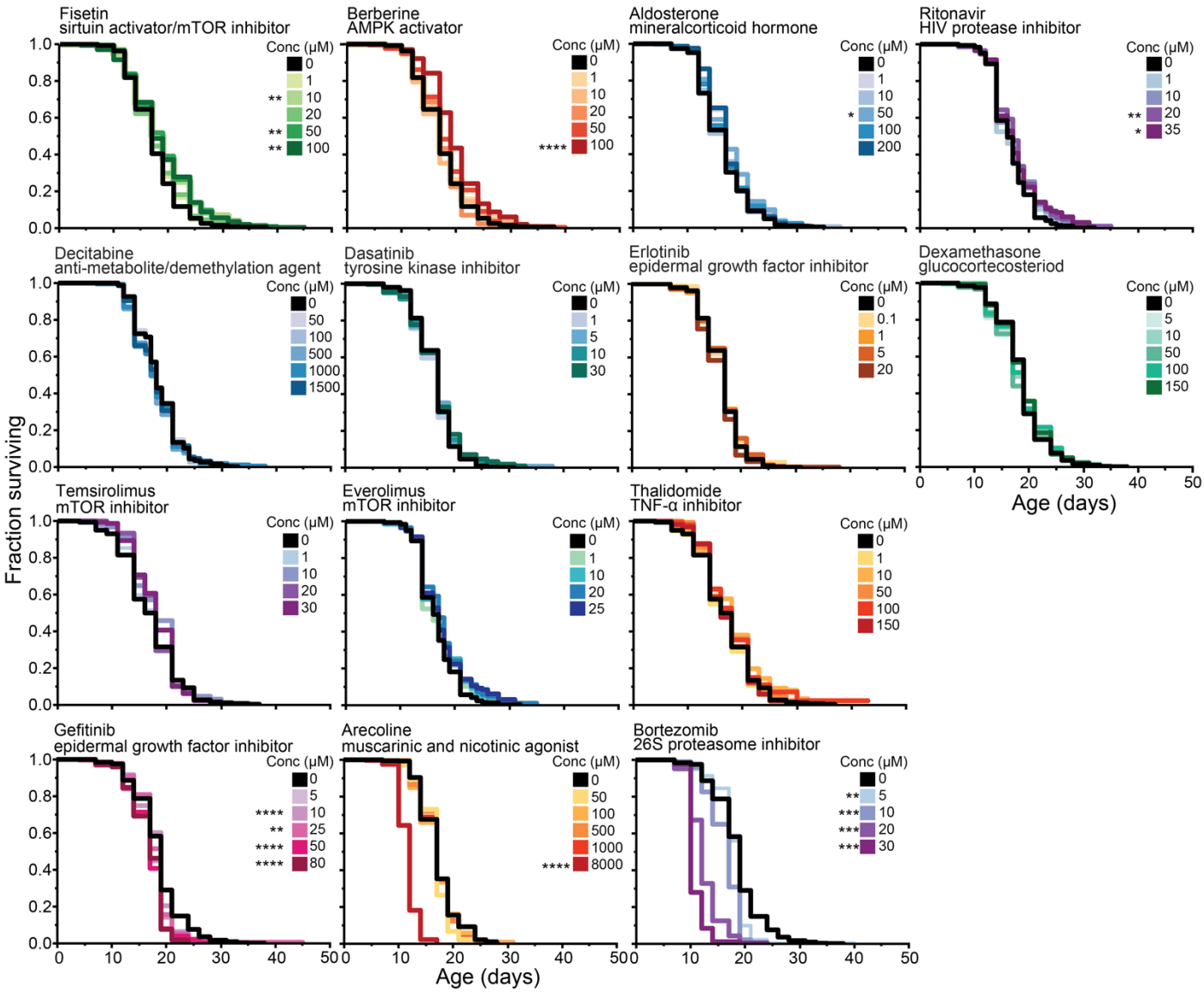

Figure 1 figure supplement 1. Longevity analysis screen in *C. elegans* N2 of 14 candidate compounds that were not selected for further study. Four compounds (fisetin, berberine, aldosterone, and ritonavir) showed a positive but non-robust lifespan effect. Seven (decitabine, dasatinib, erlotinib, dexamethasone, temsirolimus, everolimus, and thalidomide) had no significant effect on survival, and three compounds (gefitinib, arecoline, and bortezomib) showed toxic effects. Each compound was assayed at 4-5 concentrations, with the upper limit defined by solubility of the compound or toxicity. The Kaplan-Meier curves presented consist of pooled replicates from two trials. Asterisks represent *p*-values from the CPH model such that ****$p<.0001$, ***$p<.001$, **$p<.01$, and *$p<.05$.

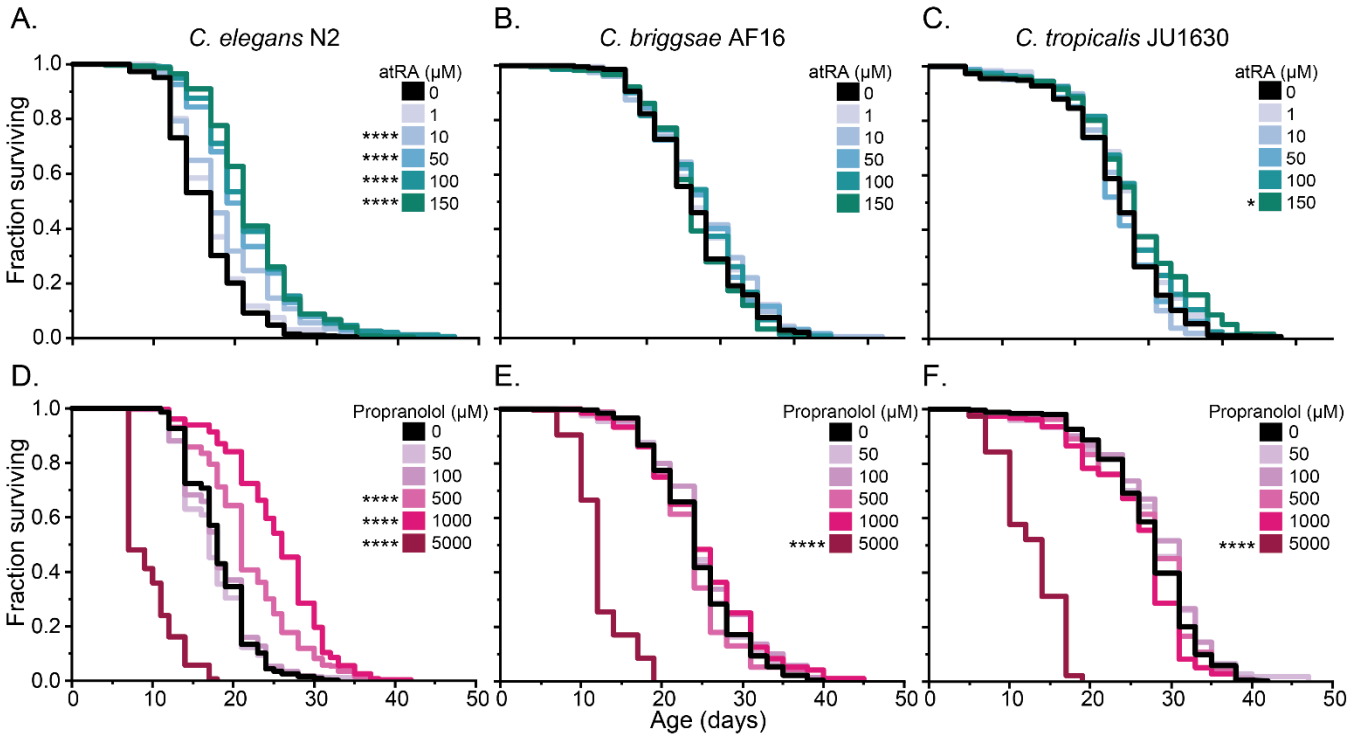

Figure 2. Dose-dependent lifespan effects of all-trans retinoic acid and propranolol across diverse *Caenorhabditis* species. (A-C) Manual lifespan analysis of five concentrations of atRA (black – DMSO control, increasing levels of teal 1 µM- 150 µM) and (D-F) propranolol (black – H_2O control, increasing levels of pink – 50-5000 µM) on three *Caenorhabditis* species. The upper limit tested was determined by compound solubility (atRA), or toxicity (propranolol). The Kaplan-Meier curves presented consist of pooled replicates from two trials. Asterisks represent *p*-values from the CPH model such that ****$p<.0001$, ***$p<.001$, **$p<.01$, and *$p<.05$.

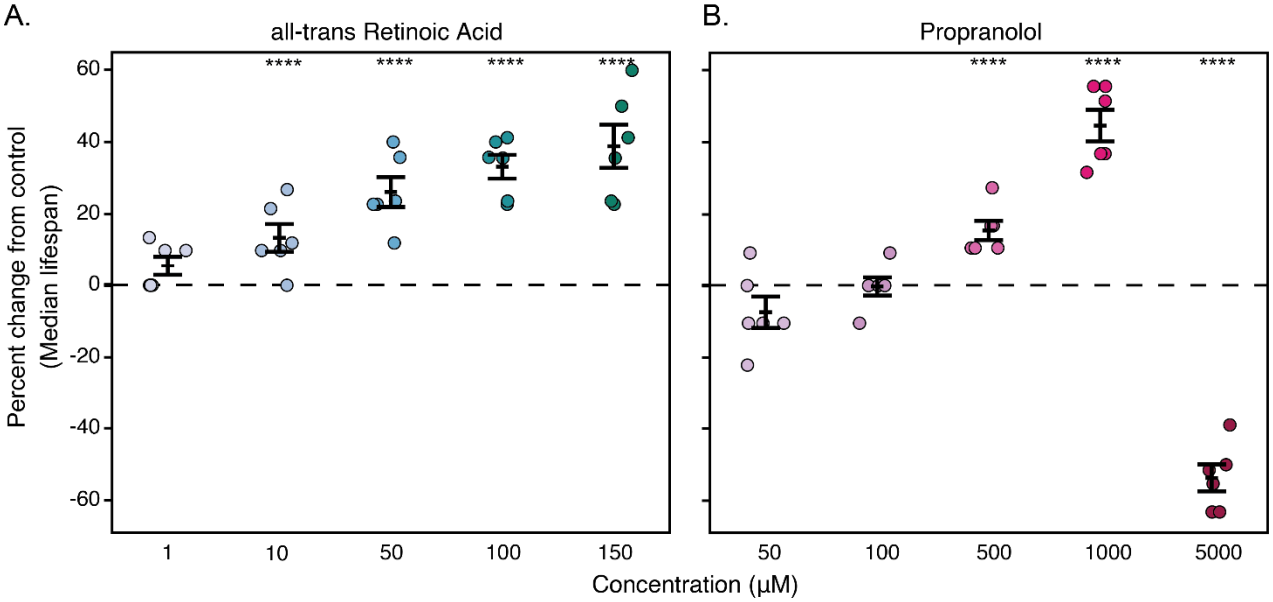

Figure 2 figure supplement 1. Median lifespan dose response of all-trans retinoic acid and propranolol in *C. elegans* N2. Percent difference in median lifespan of an individual trial plate (1-150 μM atRA, 50-5000 μM propranolol) compared to its specific control (DMSO control for atRA or H_2O for propranolol) for *C. elegans* N2 (data also presented as survival curves in figure 2 A and D). Each point represents a single plate replicate with approximately 50 worms. The error bars represent the mean +/- the standard error of the mean. Asterisks for both panels represent *p*-values from the CPH model such that ****$p<.0001$, ***$p<.001$, **$p<.01$, and *$p<.05$

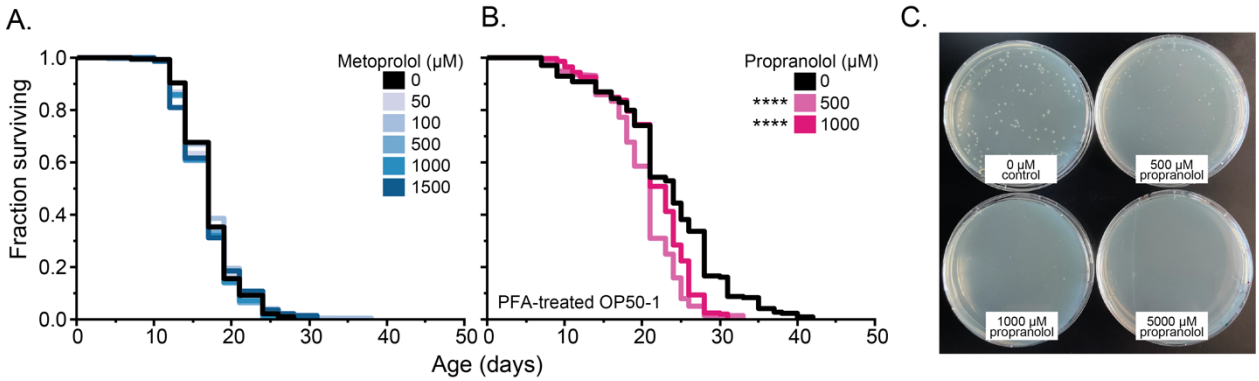

Figure 2 figure supplement 2. Metoprolol does not extend lifespan in *C. elegans*, nor does propranolol on PFA-treated OP50-1, consistent with its bacteriostatic activity. (A) Manual lifespan analysis of five concentrations of metoprolol (black – H_2O control, increasing levels of blue – 50-1500 μM) on *C. elegans* N2. (B) Manual lifespan analysis of *C. elegans* N2 on propranolol (black – H_2O control, increasing levels of pink – 500 and 1000 μM) using paraformaldehyde treated OP50-1 *E. coli.* Kaplan-Meier curves consist of pooled replicates from two trials. Asterisks represent *p*-values from the CPH model such that ****$p<.0001$, ***$p<.001$, **$p<.01$, and *$p<.05$. (C) Colony forming units of *E. coli* cultures (100 μL at a $1x10^{-6}$ dilution) on LB plates treated with H_2O, 500, 1000, and 5000 μM propranolol).

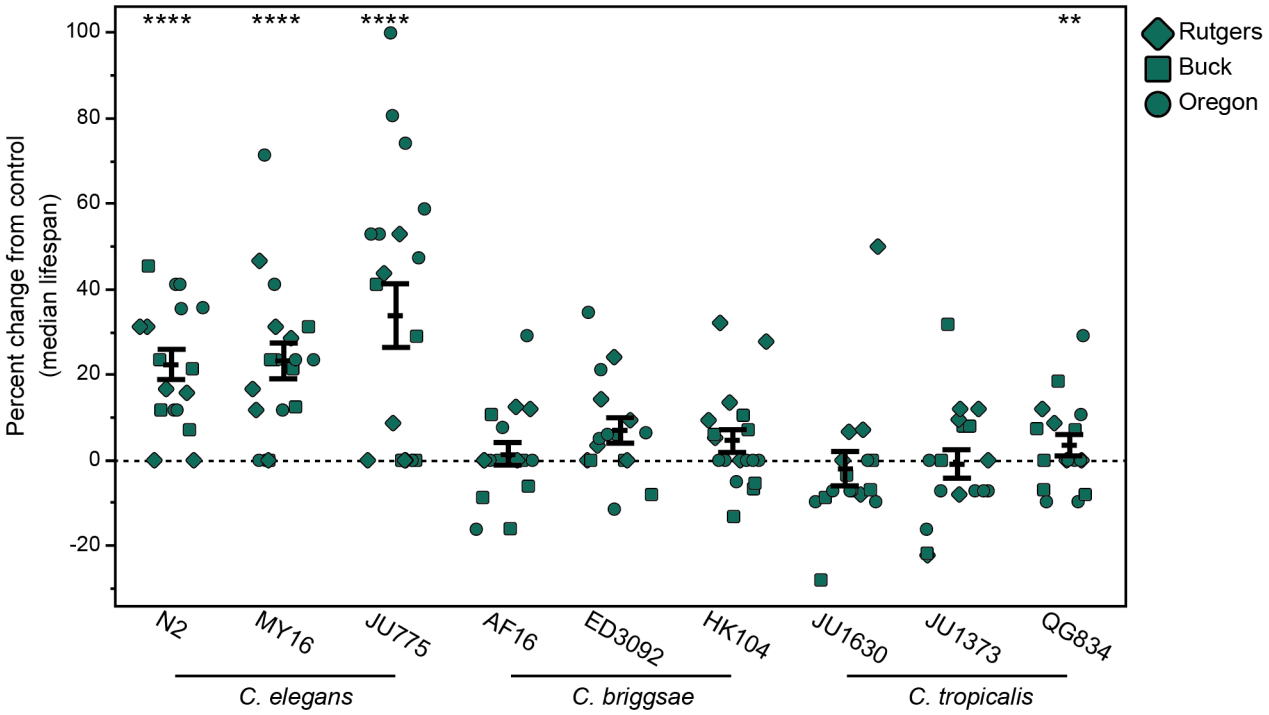

Figure 3. The vitamin A derivative atRA extends life in a species-specific manner. The effect of adult exposure to 150 µM atRA on median survival in manual lifespan assays. Three strains were tested from each of three species: *C. elegans* strains N2, JU775, and MY16, *C. briggsae* AF16, ED3092, and HK104, and *C. tropicalis* strains JU1630, JU1373, and QG834. Each point represents the percent change in median survival for an individual trial plate relative to the vehicle control median. The bars represent the mean +/- the standard error of the mean. Replicates were completed at the three CITP testing sites (circles – Oregon, squares – Buck Institute, and diamonds– Rutgers). Asterisks represent *p*-values from the CPH model such that ****$p<.0001$, ***$p<.001$, **$p<.01$, and *$p<.05$.

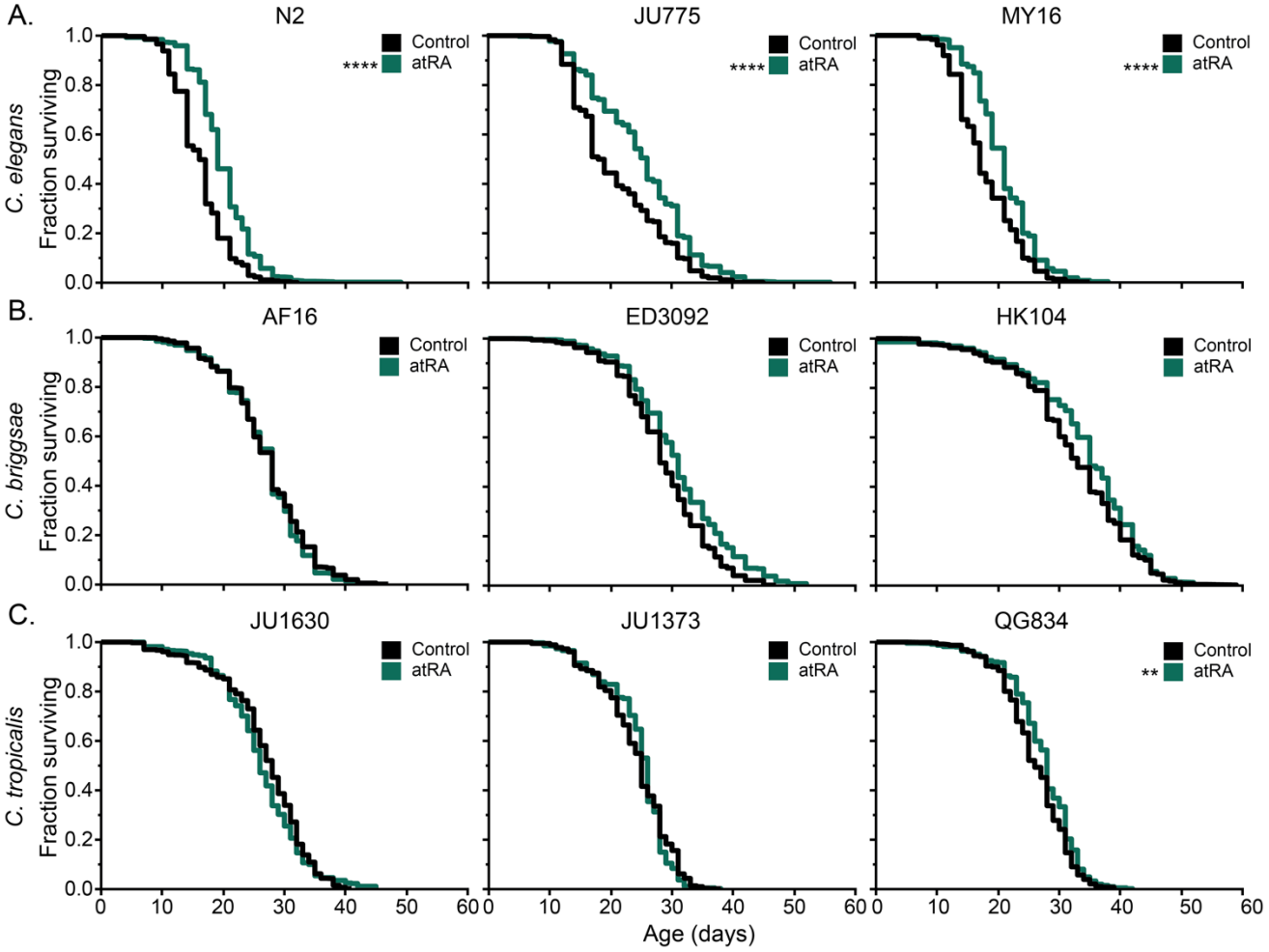

Figure 3 figure supplement 1. Lifespan curves for the data presented in figure 3 – manual survival of nine *Caenorhabditis* strains with 150 µM atRA treatment. Lifespan analysis for DMSO control (black) and 150 µM (dark teal) atRA treatment starting at day 1 of adulthood. Three *C. elegans* (N2, JU775, MY16), three *C. briggsae* (AF16, ED3092, HK104), and *C. tropicalis* (JU1630, JU1373, QG834) strains were tested. Kaplan-Meier curves represent pooled replicates from multiple trials at each of the three CITP testing sites (Oregon, Buck Institute, Rutgers). Asterisks represent *p*-values from the CPH model such that ****$p<.0001$, ***$p<.001$, **$p<.01$, and *$p<.05$

Source of Variation	
Genetic Variation	**19.7**
Among species	8.9
Among strains w/in species	8.9
Species x Compound	1.9
Strain x Compound	0
Reproducibility Among Labs	**3.8**
Lab	0
Lab x Species	0
Lab x Strain	3.4
Lab x Compound	0.4
Reproducibility Within Labs	**20.5**
Among trials	5.6
Among experimenters w/in trials	7.3
Among plates w/in experimenters	7.5
Individual Variation	**56.1**
Total	**100**

Figure 3 figure supplement 2. Pooled sources of variance for manual atRA lifespan replicated across the three CITP tested sites. Reproducibility of manual lifespan assays within and among labs of the CITP. Variance estimates were estimated using a general linear model. Bolded sources of variance categories sum the component numbers presented immediately beneath. Individual variation represents variability unassignable to a specific source of variance.

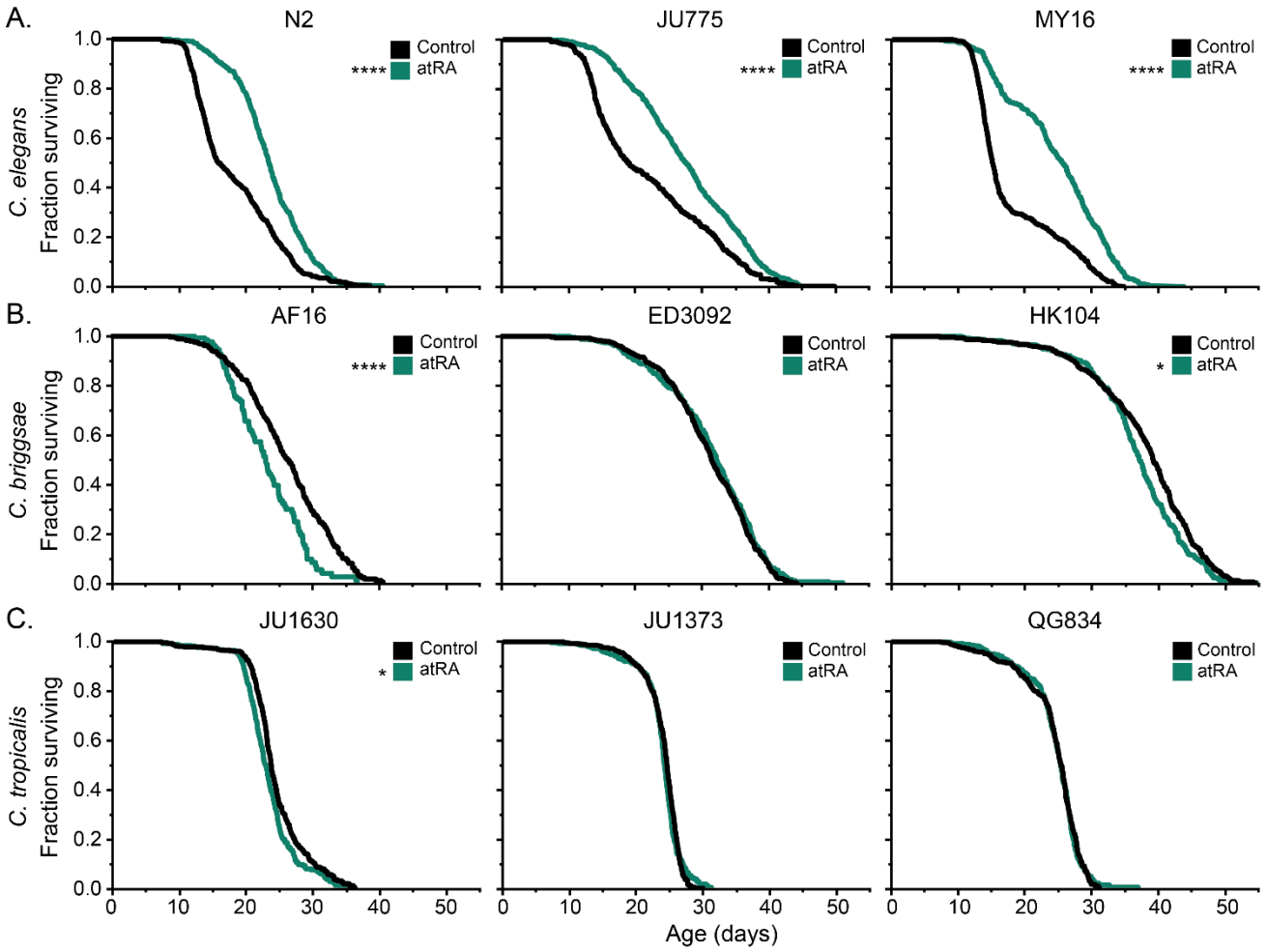

Figure 3 figure supplement 3. Survival of 9 CITP strains with atRA treatment on the ALM. Longevity analysis for control (black) and 150 µM (dark green) atRA. Three *C. elegans* (N2, JU775, MY16), three *C. briggsae* (AF16, ED3092, HK104), and *C. tropicalis* (JU1630, JU1373, QG834) strains were tested. The longevity analysis was performed using the Lifespan Machine technology (Stroustrup et al., 2013) in a single lab. Kaplan-Meier curves represent pooled replicates from at least three trials. Asterisks represent *p*-values from the CPH model such that ****$p<.0001$, ***$p<.001$, **$p<.01$, and *$p<.05$.

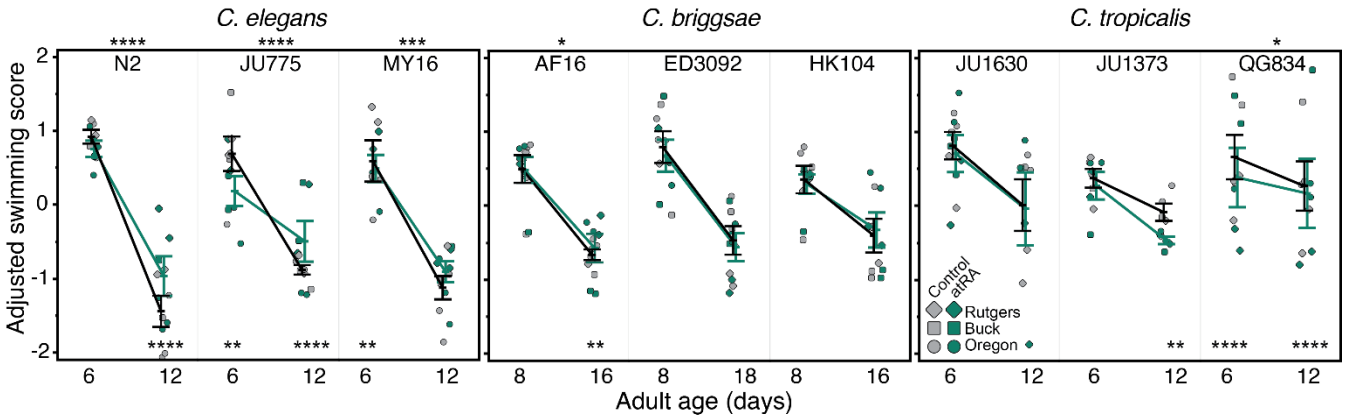

Figure 3 figure supplement 4. Swimming ability of the nine CITP strains with atRA treatment. The *C. elegans* Swim Test (CeleST) was used to assess swimming ability in all nine strains as a locomotory measure of healthspan. Eight measures of swimming ability were combined to create a single composite measure, the adjusted swimming score. Each dot represents the mean adjusted swimming score for a single trial at one of the three CITP testing sites (circle- Oregon, square- The Buck Institute, diamond- Rutgers). Bars indicate the mean +/- the standard error of the mean. Asterisks represent *p*-values from the linear mixed model such that ****$p<.0001$, ***$p<.001$, **$p<.01$, and *$p<.05$.

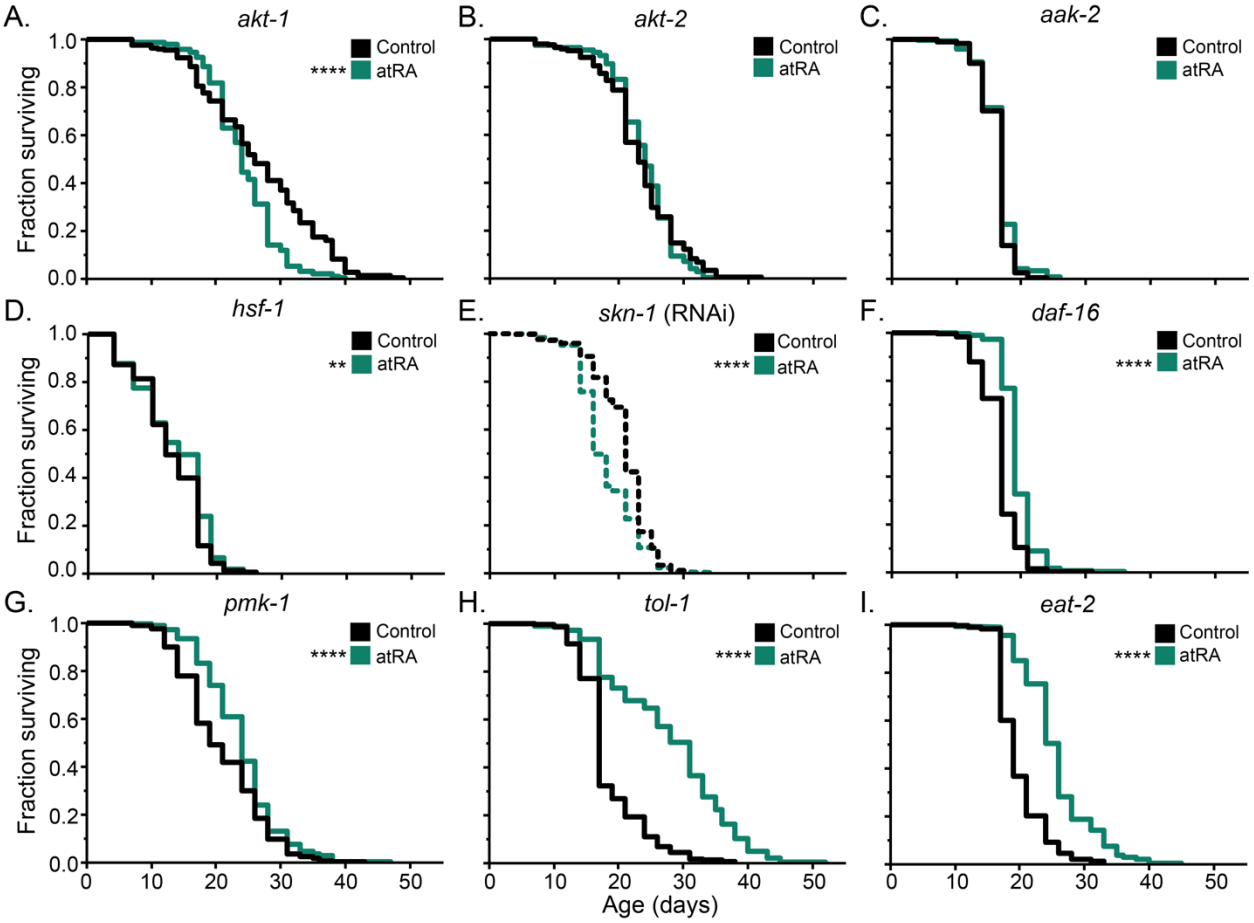

Figure 4. Genetic analysis of atRA effects on lifespan. Lifespan analysis under 150 µM atRA (green) or vehicle control (black). For wildtype, the canonical CITP N2 strain was used. This response was compared to loss of function/down regulation of: the Akt/protein kinase B (PKB) homologs (A) *akt-1* and (B) *akt-2*, (C) the AMP-activated protein kinase *aak-2*, (D) the heat shock transcription factor homolog *hsf-1*, (E) the Nrf transcription factor homolog *skn-1*, (F) the FOXO transcription factor homolog *daf-16*, (G) the p38 MAP kinase homolog *pmk-1*, (H) the toll-like receptor *tol-1*, and (I) the acetylcholine receptor *eat-2*. For *skn-1*, RNAi knock down as was used because of lethality of the mutant (see Figure 4 figure supplement 1B for control RNAi experiment). For all other genes, loss of function mutants were used. Kaplan-Meier curves include pooled replicates from two trials, except for the RNAi experiment, which consisted of three trials. Asterisks represent *p*-values from the CPH model such that ****$p<0.0001$, ***$p<0.001$, **$p<0.01$, and *$p<0.05$. (see material and methods and (Lucanic et al., 2017).

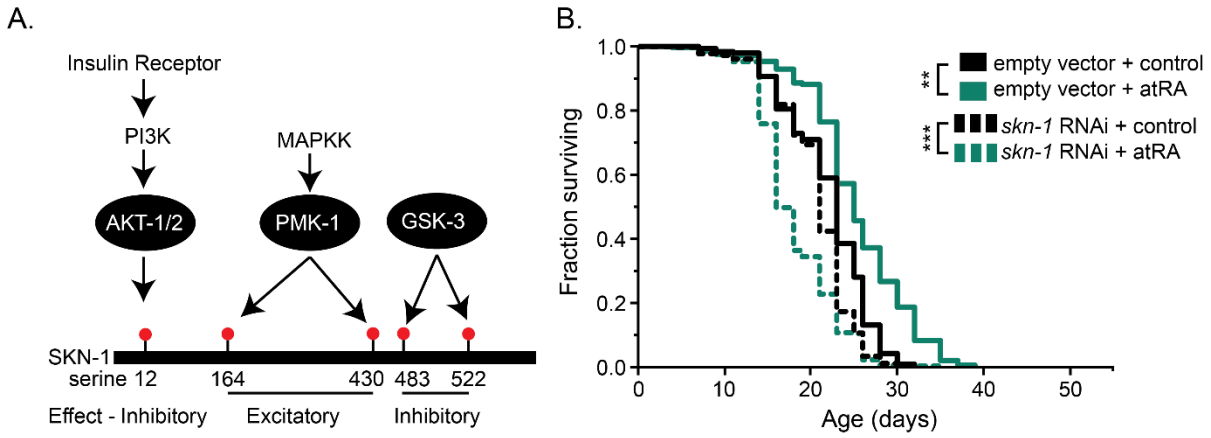

Figure 4 figure supplement 1. SKN-1 regulation and *skn-1* RNAi lifespan. (A) Post-transcriptional regulation of SKN-1 via phosphorylation is mediated by the *pmk-1*/p38 MAPK, PI3K/Akt, and GSK kinase pathways. Each pathway regulates phosphorylation of pathway-specific serines of SKN-1, enabling additive regulation. (B) Kaplan-Meier lifespan curves of worms grown on E. coli HT115 expressing either an empty vector control (solid) or *skn-1* RNAi (dashed) and treated with either 150 µM atRA (dark green) or the vehicle control (black). Each curve represents pooled replicates from three independent trials. Asterisks represent *p*-values from the CPH model such that ****$p<0.0001$, ***$p<0.001$, **$p<0.01$, and *$p<0.05$.

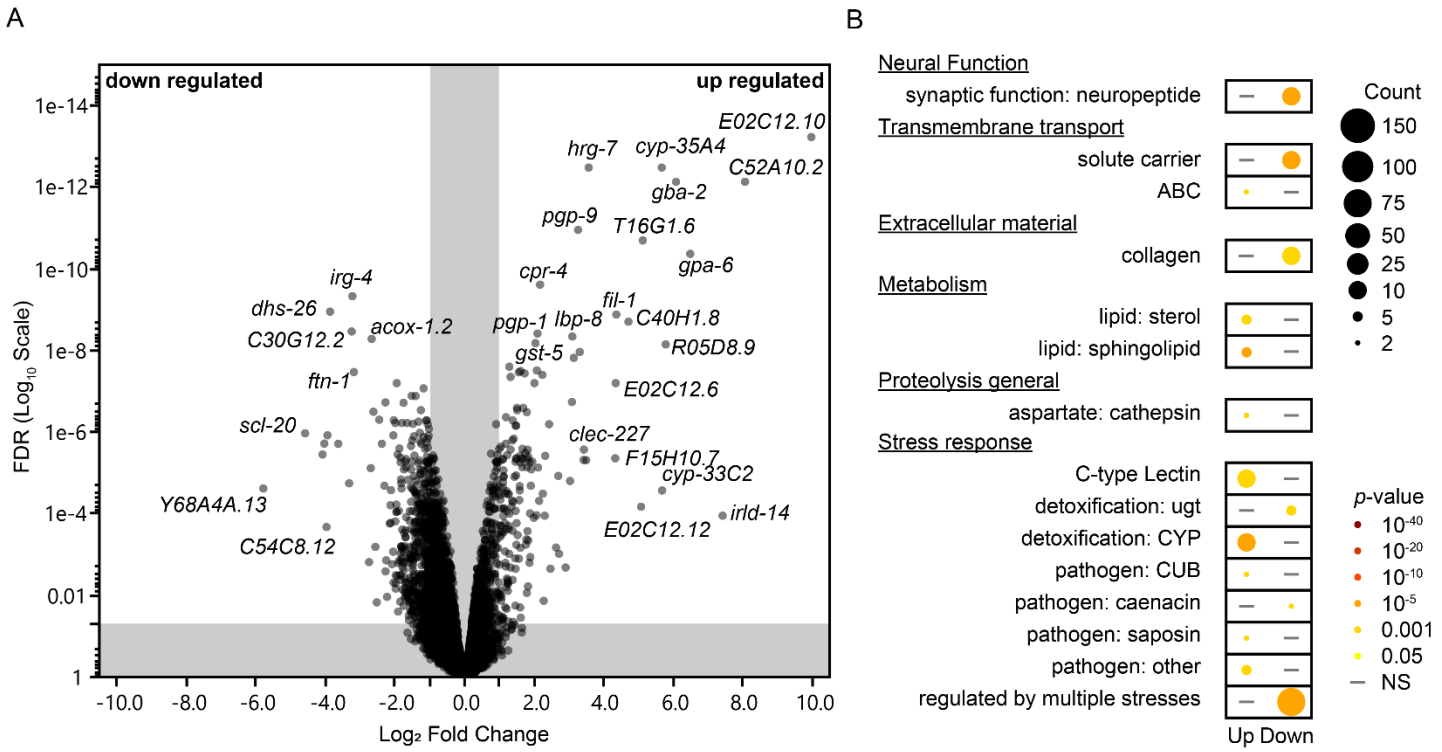

Figure 5. Altered transcriptome under atRA treatment. (A) Volcano plot for gene expression from RNAseq experiments performed on day 4 of adulthood exposed to 150 µM atRA or vehicle control. (B) Enrichment analysis using WormCat (Higgins et al., 2022; Holdorf et al., 2020).

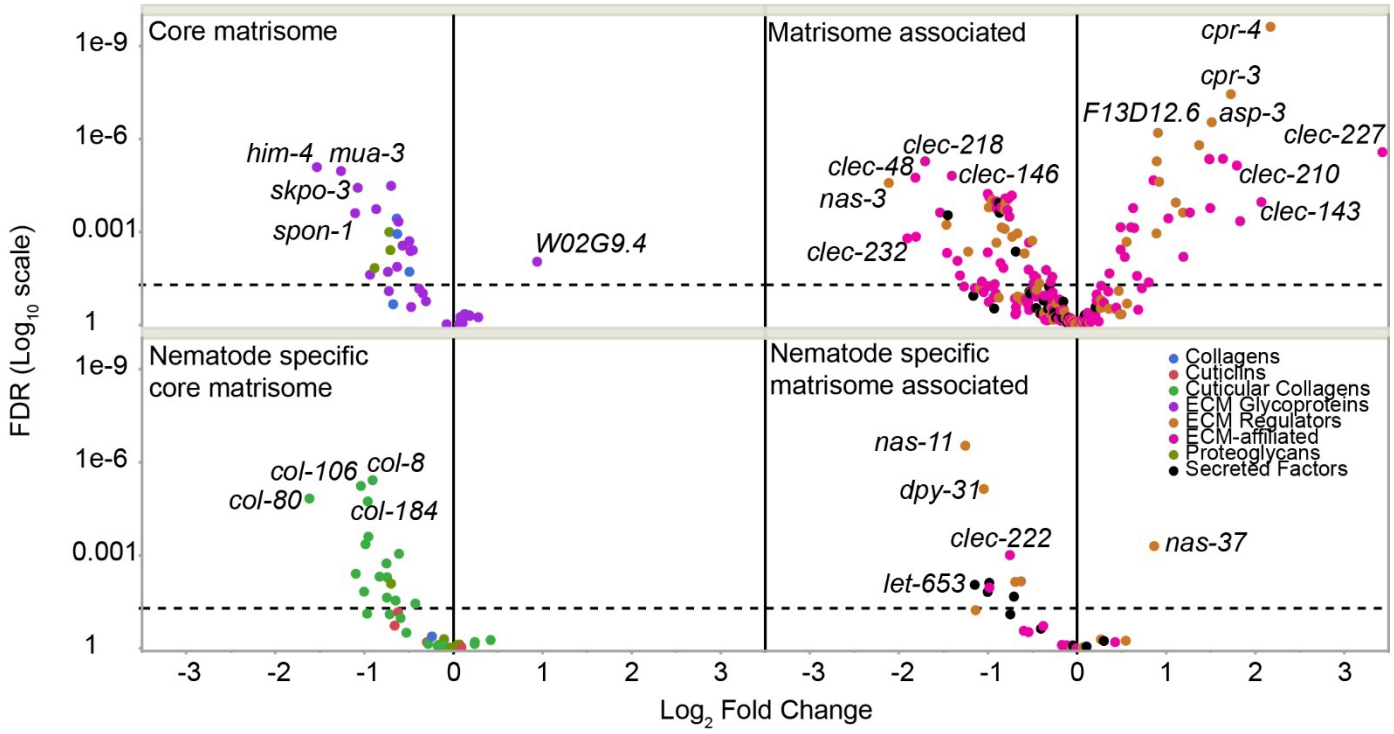

Figure 5 figure supplement 1. Collagens are downregulated in response to atRA exposure. Using a previously published *in silico* analysis of the *C. elegans* matrisome (i.e., all proteins that make up the extracellular matrix; Teuscher et al., 2019), we extracted all collagen and collagen related genes with expression data from our RNAseq dataset. For easier presentation, we used the *in silico* analysis grouping of core matrisome genes (e.g., collagens, proteoglycans, glycoproteins) and matrisome associate genes (ECM-affiliated proteins like C-type lectins, galectins, annexins, and ECM regulators like MMPs, ADAMs, and crosslinking enzymes, and secreted factors like BMPs, FGFs, and chemokines [see (Teuscher et al., 2019) and supplemental data (*Caenorhabditis* Intervention Testing Program, 2025) for a full list]). The genes were further divided into genes for which mammal to *C. elegans* orthology could be established, and those that were nematode specific.

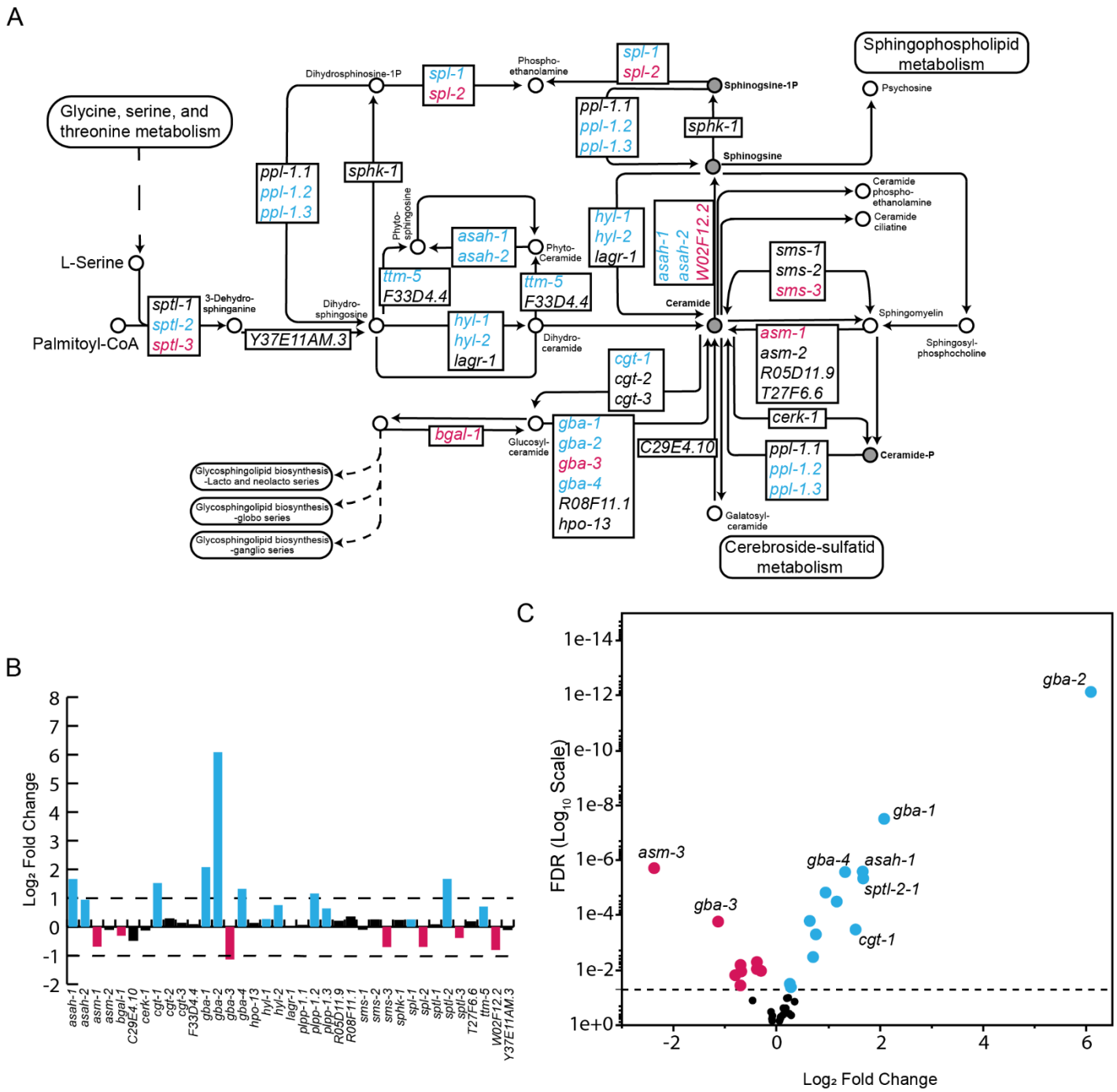

Figure 5 figure supplement 2. Effects of atRA on transcription of sphingolipid metabolism genes (A) The *C. elegans* sphingolipid metabolism network with genes significantly (FDR<.05) downregulated (red) or upregulated (blue), noted by color. (B) The log fold change for the genes and a (C) volcano plot showing the genes with their respective FDRs. All data available in supplemental information (*Caenorhabditis* Intervention Testing Program, 2025).

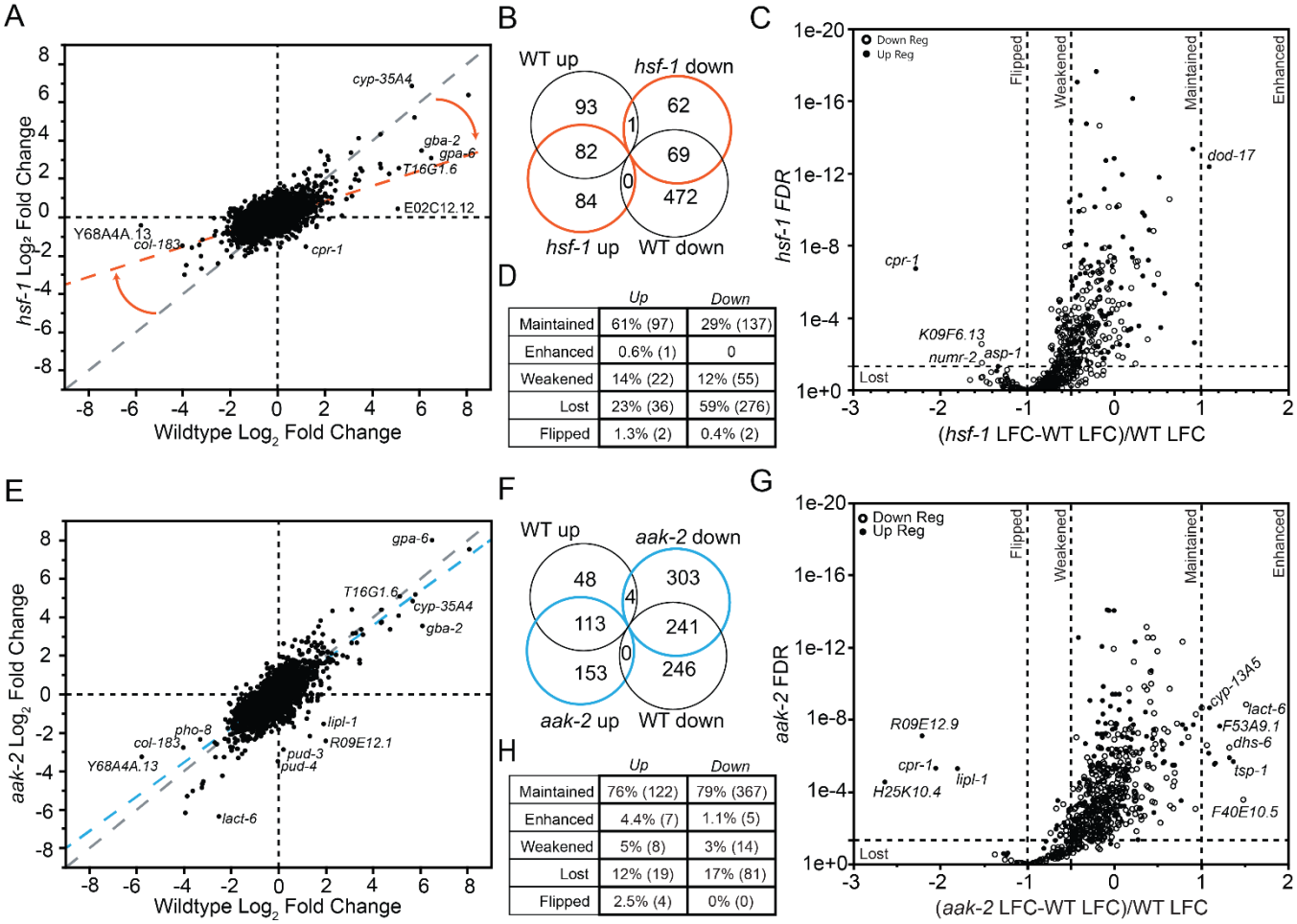

Figure 6. Analysis of the role of *hsf-1* and *aak-2* in atRA transcriptional response. (A) Comparison of DE genes with FDR<0.5 and |LFC|>1 in the *hsf-1* background to the changes observed in the wildtype background. The gray dashed line shows the expected relationship if the mutation had no effect of atRA response, while the orange dashed line shows the fit to the observed data. (B) Comparison of the genome-wide atRA induced change in expression for all genes detected in both the N2 and *hsf-1(sy441)*. (C) Plot of the FDR for the WaRGs detected in the *hsf-1(sy441)* background by the difference in expression changes between WT and mutant background normalized to the change observed in WT animals. (D) Classification of WaRGs as maintaining, weakening, losing, or flipping their response in *hsf-1(sy441)* animals. (E) Comparison of the genome-wide atRA induced change in expression for all genes detected in both the N2 and *aak-2(ok524)* datasets. The gray dashed line shows the expected relationship if the mutation had no effect of atRA response, while the blue dashed line shows the fit to the observed data. (F) Comparison of DE genes with FDR<0.5 and |LFC|>1 in the *aak-2(ok524)* background to the changes observed in the wildtype background. (G) Plot of the FDR for the WaRGs detected in the *aak-2(ok524)* background by the difference in expression change between WT and mutant background normalized to the change observed in WT animals. (H) Classification of WaRGs has maintaining, weakening, losing, or flipping their response in *aak-2(ok524)* animals.

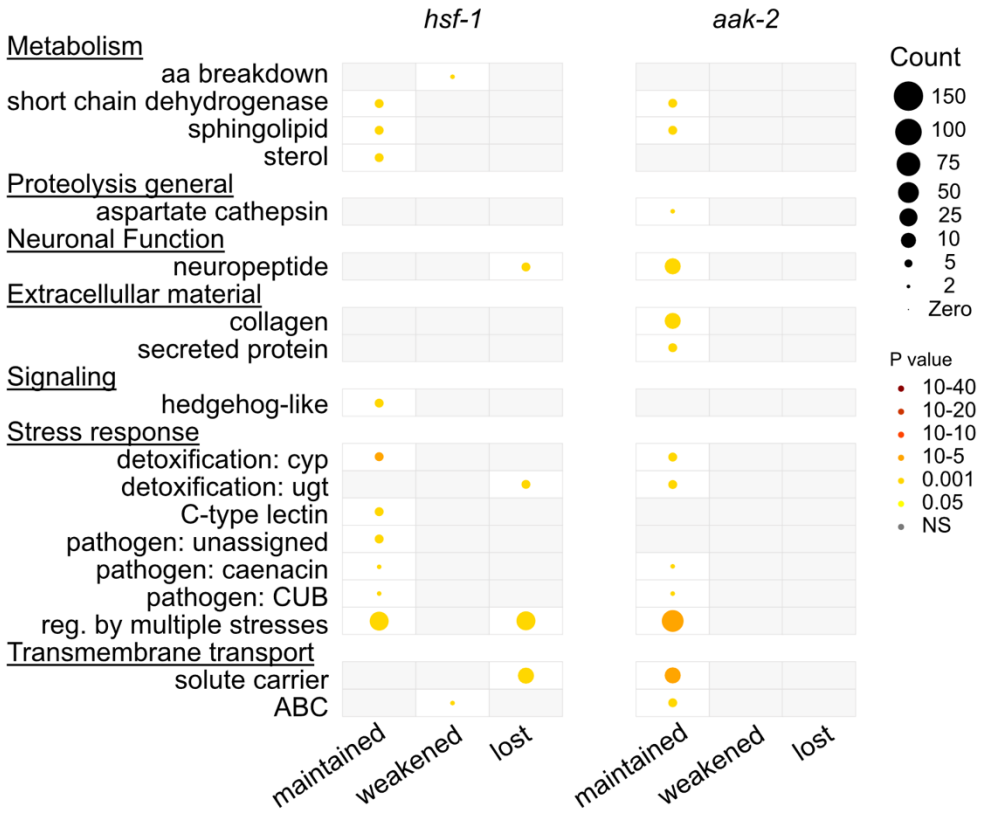

Figure 6 figure supplement 1. The WormCat enrichment analysis for the WaRGs whose response was maintained, weakened, or lost in *hsf-1(sy441)* or *aak-2(ok524)* animals.

A

	hsf-1	Maintained	Enhanced	Weakened	Lost	Flipped
aak-2		38.0%	0.2%	12.6%	48.5%	0.7%
Maintained	77.9%	208	1	68	197	1
Enhanced	3.6%	4	0	6	12	0
Weakened	1.8%	9	0	0	2	0
Lost	16.1%	9	0	2	85	2
Flipped	0.7%	2	0	1	0	1

Figure 6 figure supplement 2. (A) WaRGs response in *hsf-1(sy441)* or *aak-2* mutant backgrounds

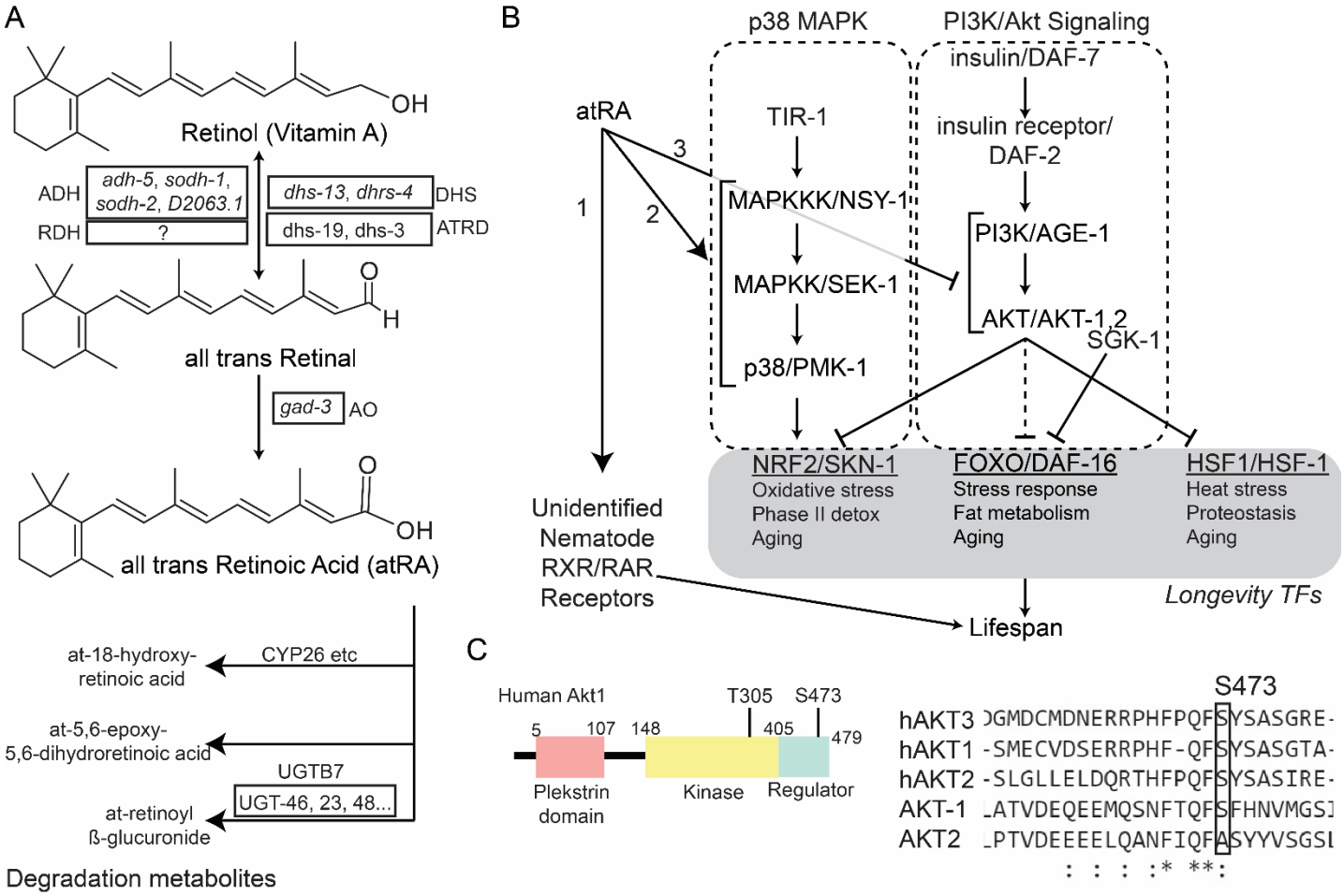

Supplemental figure 1. All-trans retinoic acid metabolism and potential regulatory roles. (A) a partial retinoic acid metabolism pathway has been identified in *C. elegans*. DHS = short chain dehydrogenase, ATRD= all-trans retinol dehydrogenase, ADH= alcohol dehydrogenase, RDH= retinal dehydrogenase. UGBT7= UDP glucuronosyltransferase family 2 member B7. AO= aldehyde oxidase. (B) atRA in mammals is known to regulate transcription through [1] retinoid binding receptors. Retinoic binding receptors are homo- or hetero- dimers that typically include at least one RXR family member. No such genes (RXR or RAR) have been identified to date in *C. elegans*. [2] Modulating p38 MAPK kinase activity, and [3] Regulating the PI3K/Akt pathway modifying the phosphorylation status of Akt. The longevity transcription factor SKN-1 is downstream of the p38 MAPK cascade in *C. elegans*. The longevity transcription factors FOXO/DAF-16, HSF1/HSF-1, and Nrf2/SKN-2 are all regulated by the IIS/PI3K/Akt pathway in C. elegans. (C) In mammals, atRA signaling through PI3K/Akt is known to involve phosphorylation of serine 473 in the human AKT genes within minutes of atRA treatment. The serine is conserved in *C. elegans akt-1*.